Journal of Asian Earth Sciences 154 (2018) 162–186

Contents lists available at ScienceDirect

Journal of Asian Earth Sciences

journal homepage: www.elsevier.com/locate/jseaes

Full length article

A synthesis of magmatic Ni-Cu-(PGE) sulfide deposits in the ~260 Ma Emeishan large igneous province, SW China and northern Vietnam

Christina Yan Wang[a,*], Bo Wei[a], Mei-Fu Zhou[b], Dinh Huu Minh[c], Liang Qi[d]

[a] Key Laboratory of Mineralogy and Metallogeny, Guangzhou Institute of Geochemistry, Chinese Academy of Sciences, Guangzhou 510640, China
[b] Department of Earth Sciences, The University of Hong Kong, Hong Kong, China
[c] Asian Mineral Resources, Ba Dinh District, Hanoi, Viet Nam
[d] State Key Laboratory of Ore Deposit Geochemistry, Institute of Geochemistry, Chinese Academy of Sciences, Guiyang 550002, China

ARTICLE INFO

Keywords:
Ni-Cu-(PGE) sulfide mineralization
Mantle source
Crustal contamination
Magma plumbing system
Emeishan large igneous province

ABSTRACT

Magmatic Ni-Cu-(PGE) sulfide deposits in the ca. 260-Ma Emeishan large igneous province (LIP) are all hosted in relatively small, mafic-ultramafic intrusions with surface areas usually less than 1 km^2. These deposits are mainly distributed in the Danba, Panzhihua-Xichang (Panxi), Huili, Yuanmou, Midu, Funing and Jinping regions in SW China and the Ta Khoa region in northern Vietnam. They include Ni-Cu-(PGE) sulfide-dominated, Ni-Cu sulfide-dominated, and PGE-dominated types. Sulfide ores of the Ni-Cu-(PGE) and Ni-Cu sulfide-dominated deposits contain more than 10 vol% sulfides and have low PGE concentrations relative to the ores that contain < 3 vol% sulfides in the PGE-dominated deposits. The parental magmas of the host mafic-ultramafic intrusions may have been derived primarily from low-Ti picritic magmas that were produced by high degrees of partial melting of a depleted mantle source. The primary low-Ti picrites of the Emeishan LIP have relatively restricted εNd(t) and γOs(t) isotopic compositions, however, some of the host intrusions exhibit a large range of both εNd(t) (−9.5 to +0.8) and γOs(t) (+5.4 to +77), indicating that they experienced variable degrees of crustal contamination during emplacement. In addition, sulfides from sulfide ores of the Ban Phuc intrusion in northern Vietnam and those from sulfide veins in country rocks have $\delta^{34}S$ values ranging from −6.7 to −3.4‰, whereas sulfides from sulfide ores of the Baimazhai No.3, Yingpanjie, Jinbaoshan and Nantianwan intrusions in SW China have highly variable $\delta^{34}S$ ranging from −0.2 to +21.4‰, indicating the addition of crustal sulfur into the mantle-derived mafic magmas. Platinum-group minerals (PGM) are abundant in the Ni-Cu-(PGE) sulfide-bearing intrusions, and they span a wide range of composition. More than 130 PGM grains have been identified in the Pt-Pd-rich Jinbaoshan intrusion, whereas only one small froodite ($PdBi_2$) grain was observed in the Ni-Cu sulfide-dominated Baimazhai No. 3 intrusion. Overall, the three types of Ni-Cu-(PGE) sulfide deposits in the Emeishan LIP can be taken as a spectrum of Ni-Cu-(PGE) sulfide mineralization, the formation of which involved similar magmatic processes in open systems of magma conduits. The magma conduits developed along the cross-linking structures created by numerous strike-slip faults and each intrusion appears to be part of a connecting trellis of conduits that formed complex pathways from the mantle to the surface. The Ni-Cu sulfide-dominated deposits are attributed to a single sulfide segregation event in staging magma chambers, whereas the PGE-dominated deposits were likely formed by a multistage-dissolution, upgrading process in the staging chambers. The Ni-Cu-(PGE) sulfide-dominated deposits may have experienced interaction between successive pulses of S-undersaturated mafic magma and early segregated sulfide melts in the staging chambers. This study is intended to provide a better understanding of the magmatic processes related to the formation of conduit-type Ni-Cu-(PGE) sulfide deposits associated with continental flood basalt magmatism.

1. Introduction

Large igneous provinces (LIPs) are recognized as tremendous reservoirs of magmatic Ni-Cu-(PGE) sulfide, Fe-Ti oxide and chromite deposits (Naldrett, 1997, 2010a; Pirajno, 2000; Schissel and Smail, 2001; Ernst and Jowitt, 2013). Magmatic Ni-Cu-(PGE) sulfide deposits that are hosted in mafic-ultramafic intrusions related to LIPs are the dominant sources of Ni and PGEs in the world (Naldrett, 1997, 2010a, 2010b; Pirajno, 2000; Schissel and Smail, 2001; Mudd, 2012; Ernst and Jowitt, 2013). They can be generally divided into two groups; Ni-Cu

* Corresponding author.
E-mail address: wang_yan@gig.ac.cn (C.Y. Wang).

https://doi.org/10.1016/j.jseaes.2017.12.024
Received 15 September 2017; Received in revised form 22 November 2017; Accepted 12 December 2017
Available online 13 December 2017

sulfide-dominated deposits with PGEs as by-products, and PGE-dominated and Ni-Cu sulfide-poor deposits (e.g., Naldrett, 2004). One of the most important Ni-Cu sulfide-dominated deposits is hosted in the Noril'sk-Talnakh intrusions associated with the end-Permian Siberian Traps in Russia (Naldrett, 1992; Hawkesworth et al., 1995; Arndt et al., 2003; Lightfoot and Keays, 2005). Other examples include a number of deposits hosted in small-scale, mafic-ultramafic intrusions in the Emeishan LIP (Glotov et al., 2001; Wang et al., 2007; Song et al., 2008b; Zhou et al., 2008), and those in the Duluth Complex and other intrusions in the Keweenawan LIP in the United States (Miller and Ripley, 1996). PGE-dominated deposits can be hosted in large layered intrusions such as the Bushveld Complex in South Africa (Naldrett, 2004, 2010a) or in small sills such as those in the Emeishan LIP in SW China (Wang et al., 2010; Tang et al., 2013). However, magmatic Ni-Cu-(PGE) sulfide deposits worldwide have highly variable Ni, Cu and PGE tenors (Naldrett, 2011). For example, the deposits in the Emeishan LIP are far less economically important than those hosted in the Bushveld Complex and Noril'sk-Talnakh intrusions in both the tenor of metals and the size of ore bodies.

Major Ni-Cu-(PGE) sulfide-bearing, mafic-ultramafic intrusions in the Emeishan LIP, except for the Ban Phuc intrusion in northern Vietnam, have been well documented in a number of earlier studies over the past decade (e.g., Glotov et al., 2001; Song et al., 2003; Wang et al., 2006; Tao et al., 2008; Wang et al., 2010; Zhu et al., 2012; Tang et al., 2013). It is now timely to summarize some common features of these mafic-ultramafic intrusions and to evaluate the major factors controlling Ni-Cu-(PGE) sulfide mineralization, e.g., nature of mantle sources, role of crustal contamination, addition of external crustal sulfur, and magmatic processes in dynamic magma conduits.

In this paper, we compile available data from the literature for chalcophile elements, Nd-Os isotopic compositions and major platinum-group minerals of Ni-Cu-(PGE) sulfide-bearing, mafic-ultramafic intrusions in SW China, and present our new data for the Ban Phuc intrusion in northern Vietnam. We have also obtained *in situ* S isotopic compositions of sulfides from the ores and rocks of both Ni-Cu-(PGE) sulfide- and Fe-Ti oxide-bearing mafic-ultramafic intrusions in the Emeishan LIP. On the basis of literature sources and our new data, we conclude that these Ni-Cu-(PGE) sulfide-bearing intrusions may have been derived primarily from low-Ti picritic magmas related to the Emeishan mantle plume and that they experienced similar magmatic processes in open-system magma conduits. Remarkably different sulfide contents and chalcophile element concentrations of sulfide ores from different deposits are mainly related to the amounts of S-undersaturated, mafic magma that flowed through staging magma chambers and its interaction with early segregated sulfide melts in the chambers.

2. Geological background

The Emeishan LIP occurs in SW China and northern Vietnam. The part in SW China is located in the western margin of the Yangtze Block and the eastern part of the Tibetan Plateau (Chung and Jahn, 1995), and is bounded to the southwest by the Ailao Shan-Red River shear zone (Fig. 1). The part in northern Vietnam is considered to be detached from main occurrence in SW China due to left-lateral displacement on the Ailao Shan–Red River shear zone in the Cenozoic with a total offset of ~600 km (Chung et al., 1997, 1998; Hanski et al., 2004; Ali et al., 2010).

The Emeishan LIP is composed dominantly of volcanic rocks with numerous mafic-ultramafic intrusions and felsic plutons. The flood basalts are believed to have been derived from a mantle plume at ca. 260 Ma (Chung et al., 1998; Xu et al., 2001; Zhou et al., 2002). The volcanic succession is up to ~5 km thick and is underlain by limestone of the middle Permian Maokou Formation and overlain by shale and volcaniclastic rocks of the late Permian Xuanwei Formation, which is a continental facies in places. A domal structure is considered to have existed prior to eruption of the flood basalts (He et al., 2003) and to have divided the Emeishan LIP into an inner zone, intermediate zone and outer zone, a division supported by thickness variations of the Maokou Formation, the extent of erosion, thickness variations and chemistry of the volcanic rocks and the crust-mantle structure (Xu et al., 2004).

The volcanic succession of the Emeishan LIP comprises low-Ti and high-Ti flood basalts, along with minor amounts of picrite, andesite and rhyolite (Song et al., 2001, 2008a; Xu et al., 2001; Xiao et al., 2003, 2004; Hanski et al., 2004, 2010; Zhou et al., 2006; Wang et al., 2007; Qi and Zhou, 2008; Li et al., 2010). In the Panxi region, the central part of the Emeishan LIP, there are mainly high-Ti basalts with minor amounts of tephrite and basaltic andesite (Mei et al., 2003; Qi et al., 2008). To the north, Permian lavas in the Danba and Litang regions are mainly high-Ti basalts and andesite (Song et al., 2004a), whereas to the southwest, high-Ti picritic lavas also occur in the Dali, Binchuan, Yongsheng and Lijiang regions (Ren et al., 2017). Farther to the southwest, the flood basalts in the Jinping region in China and Song Da region in Vietnam occur as a ~300-km-long belt emanating from the southernmost part of the Emeishan LIP. These lavas are composed of high-Ti and low-Ti basalts, low-Ti picrite and minor amounts of rhyolite (Xiao et al., 2003; Hanski et al., 2004; Wang et al., 2007; Anh et al., 2011). In two recent studies, Permian flood basalts were also found in areas outside the previously defined Emeishan LIP, such as high-Ti basalts in the western part of Guangxi Province in SW China (Liu et al., 2017b) and massive pyroxene-plagioclase-phyric, high-Ti basaltic lavas in the Yanghe region in the northeastern part of the Sichuan Basin (Li et al., 2017). These new findings show that the Emeishan LIP originally extended over an area of up to 7×10^5 km^2 (Li et al., 2017 and references therein) (inset in Fig. 1), instead of 5×10^5 km^2 as suggested in earlier studies (Xiao et al., 2004).

There are many mafic-ultramafic, layered intrusions in the Emeishan LIP. Some of them host world-class magmatic Fe-Ti-(V) oxide deposits and others host Ni-Cu-(PGE) sulfide deposits. The largest Fe-Ti-oxide deposits are mainly distributed in the Panxi region along major N-S-trending faults (Fig. 1), including those at Taihe, Xinjie, Baima, Hongge, Panzhihua and Anyi. These deposits constitute a mineralized belt ~400 km long and 10–30 km wide and form the most important metallogenic district for Fe, Ti and V in China (Zhou et al., 2005, 2013). The host intrusions are mainly composed of gabbro with variable amounts of ultramafic rocks and are mostly dated to be ca. 260 Ma using high-precision zircon U-Pb dating methods (Zhou et al., 2013 and references therein). In the southwestern part of the Emeishan LIP, the Fe-Ti oxide-bearing Mianhuadi mafic-ultramafic complex occurs in the Red River fault zone near the border of China and Vietnam. The intrusion has undergone granulite facies metamorphism (Liu et al., 2017a) but the protolith is well constrained to be part of the Emeishan LIP with a protolith age of ca. 260 Ma (Zhou et al., 2013).

Mafic-ultramafic sills/intrusions in the Emeishan LIP that host Ni-Cu-(PGE) sulfide deposits are mainly distributed in the Danba, Huili, Panxi, Yuanmou, Funing, Midu, Jinping and Ta Khoa regions (Song et al., 2003, 2006, 2008b; Wang and Zhou, 2006; Zhou et al., 2006; Tao et al., 2007, 2010; Wang et al., 2010, 2011, 2012a,b) (Fig. 1). Although these deposits are economically important and some of them have been mined for Ni and Cu, they are generally small in size (Table 1). Several Ni-Cu-(PGE) sulfide-bearing, mafic-ultramafic intrusions have been dated using the SHRIMP zircon U-Pb dating technique (Fig. 2a). Gabbros from the Baimazhai No.3 intrusion in the Jinping region contain zircon grains with an age of 258.5 ± 3.5 Ma (Wang et al., 2006), similar to the Re–Os isochron age of 259 ± 20 Ma for massive sulfide ores of the intrusion (Sun et al., 2008). Zircon grains from wehrlite of the Jinbaoshan intrusion in the Midu region, western part of the Emeishan LIP, yielded an age of 260.6 ± 3.5 Ma and those from the associated gabbro yielded an age of 260.7 ± 5.6 Ma (Tao et al., 2009). In the central part of the Emeishan LIP, gabbros from the Limahe intrusion in the Huili region have zircon grains with an age of 263 ± 3 Ma (Zhou et al., 2008), and diorites from the Zhubu intrusion

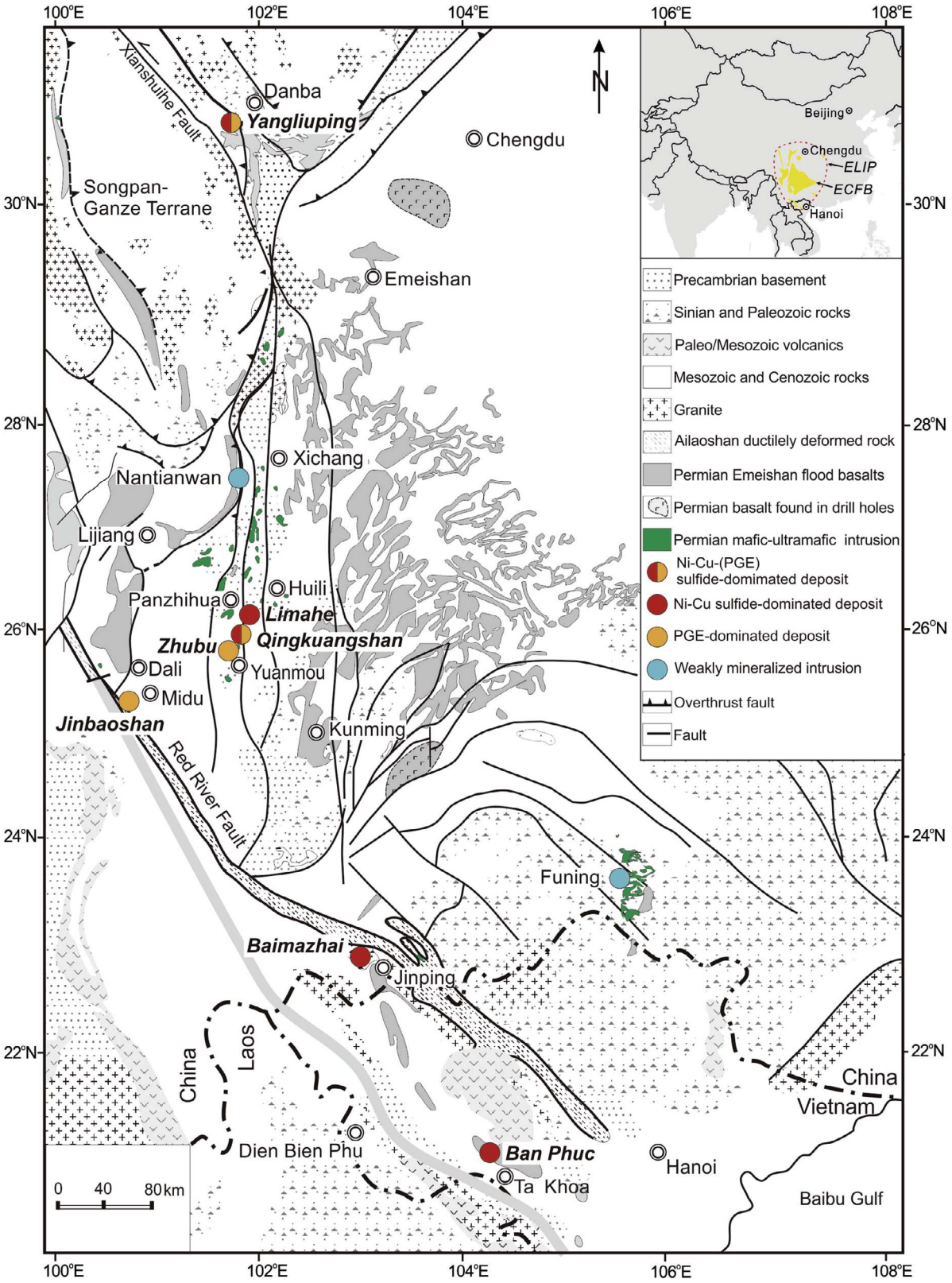

Fig. 1. Regional geological map showing the distribution of Emeishan continental flood basalts (ECFB) and associated mafic–ultramafic intrusions in the Emeishan large igneous province (ELIP) in SW China and northern Vietnam (modified after Wang et al., 2005). The inset is modified after Xu et al. (2001) and Li et al. (2017).

Table 1
Summary of major features of the Ni-Cu-(PGE) sulfide-bearing mafic-ultramafic intrusions in the Emeishan LIP.

Intrusions	Location	Morphology	Rock types	Country rocks	Surface area	Ore reserves	References
Yangliuping	Danba, Sichuan Province, China	Sill, 200–300 m thick and 1000–2000 m in strike length	Altered peridotite, olivine websterite, olivine clinopyroxenite, and gabbro	Middle Devonian graphite-bearing schist, slate and graphite-bearing marble of the Weiguan Formation	0.6 km^2	100,000 tons of Ni@ 0.45 wt% Ni, 63,000 tons of Cu@0.16 wt% Cu, and 17 tons of PGE@ 0.55 ppm total PGE	Song et al. (2003) and Song et al. (2004b)
Qingkuangshan	Huili, Sichuan Province, China	Dyke-like body and funnel-shaped in cross section, about 200 m long, 20–50 m wide, and vertical downward extension 150–180 m	peridotite, wehrlite, pyroxenite, gabbro	Mesoproterozoic mica schist of the Hekou Formation	0.1 km^2		Zhu et al. (2012)
Limahe	Huili, Sichuan Province, China	Elongate rhomboid-shaped body. ~900 m long and 180 m wide on surface, vertical downward extension over 200 m	wehrlite, olivine websterite, gabbro, diorite	Neoproterozoic pyrite-bearing quartzites, graphitic slates, and siliceous limestones of the Huili Formation	1.8 km^2	3 Mt ore @ 1 wt% Ni and 0.6 wt% Cu	Tao et al. (2008) and Tao et al. (2010)
Baimazhai	Jinping, Yunnan Province, China	Concentrically zoned body and lens-like in cross section. 530 m in length, 190 m in width and 24–64 m in thickness	orthopyroxentie, gabbro, websterite	Ordovician sandstone and slate of the Xiangyang Formation	0.1 km^2	50,000 tonnes of Ni; Ni 1.03 wt%, Cu 0.81 wt	Wang and Zhou (2006) and Wang et al. (2006)
Ban Phuc	Song Da, Vietnam	Elongate lenticular-shaped and funnel-shaped in cross section	dunite, wehrlite	Devonian schist, quartzite, and amphibolite of the Ta Hoa Formation	1 km^2	119,400 tonnes of Ni, 40,500 tonnes of Cu	Glotov et al. (2001)
Jinbaoshan	Midu, Yunnan Province, China	Sill-like body. 4760 m long, 760–1240 m wide, and 8–170 m thick	wehrlite, gabbro	Devonian dolomite, sandstone and slate of the Jinbaoshan Formation	5 km^2	1 Mt @ 3.0 ppm (Pd + Pt)	Tao et al. (2007), Wang et al. (2008) and Wang et al. (2010)
Zhubu	Yuanmou, Yunnan Province, China	Elliptical shape, and curved cone-like in cross section. ~750 m long and ~400 m wide on surface and downward extension over 580 m	lherzolite, olivine websterite, gabbro, gabbrodiorite	Precambrian gneiss of the Yuanmou Formation	0.3 km^2	3.0 ppm (Pd + Pt)	Zhu et al. (2007) and Tang et al. (2013)

in the Yuanmou region have a zircon U-Pb age of 261 ± 1 Ma (Zhou et al., 2008). The Nantianwan intrusion in the Panxi region, which has potentially important Ni-Cu sulfide mineralization (Wang et al., 2012a,b), has been dated at 263.4 ± 2.0 Ma using zircon from gabbronorite (Wang et al., 2012a).

In this study, we separated zircon grains from diorites of the Ban Phuc intrusion in the Ta Khoa region, northern Vietnam. Among 21 analyzed zircons, four with high U (U > 5000 ppm), yielded significantly older ages (267–278 Ma) than the others (Table 2) and these were excluded. The remaining 17 grains have ages ranging from 253 ± 3.4 to 264 ± 3.1 Ma and yielded an average $^{206}Pb/^{238}U$ age of 259.9 ± 1.5 Ma with a MSWD of 1.42 (Fig. 2b). Thus, the Ban Phuc intrusion is considered to have a crystallization age of ca. 260 Ma, similar to that of mafic-ultramafic intrusions elsewhere in the Emeishan LIP.

3. Magmatic Ni-Cu-(PGE) sulfide deposits in the Emeishan LIP

Ni-Cu-(PGE) sulfide deposits in the Emeishan LIP form three major groups, i.e., Ni-Cu-(PGE) sulfide-dominated, Ni-Cu sulfide-dominated, and PGE-dominated (Song et al., 2008b). The first group [Ni-Cu-(PGE) sulfide-dominated] includes the Yangliuping and Qingkuangshan deposits, whereas the second group (Ni-Cu sulfide-dominated) includes the Limahe, Baimazhai and Ban Phuc deposits and the Nantianwan intrusion with potential Ni-Cu sulfide-dominated mineralization. The third group (PGE-dominated) includes the Jinbaoshan and Zhubu deposits. The metal reserves and PGE tenors for each of these deposits are listed in Table 1.

3.1. Ni-Cu-(PGE) sulfide-dominated intrusions

3.1.1. Yangliuping intrusion

The geology of the Yangliuping intrusion in the Danba region, Sichuan Province (Fig. 1), has been described by Song et al. (2003, 2008b). The Yangliuping intrusion is located in the core of the Yangliuping dome in the southeastern part of the Mesozoic Songpan-Ganzi orogenic belt (Yan et al., 2003). The Yangliuping dome consists of Devonian to Triassic strata (Fig. 3) that underwent greenschist facies metamorphism in the late Triassic (Arne et al., 1997). The Devonian strata consist of mica-quartz schist, mica schist, quartzite, slate, graphite-bearing schist and graphite-bearing marble with abundant pyrite (up to 5%). The overlying Carboniferous strata are mainly composed of calcareous slate and mica schist. Early Permian strata conformably overlie the Carboniferous strata and include marble with slate intercalations. The late Middle Permian volcanic rocks of the Dashibao Formation, which are ~500–1500 m thick, are composed of basaltic tuff, basaltic agglomerate and rare pillow lavas that host Ni-Cu-(PGE) sulfide-bearing sills (Song et al., 2003). The Dashibao Formation is overlain conformably by Permian metamorphosed sandstone and tuff. The Triassic clastic rocks conformably overlie the late Permian strata.

There are four mineralized mafic-ultramafic intrusions, Yangliuping, Zhengziyanwuo, Xiezuoping and Daqiangyanwo, in the core of the Yangliuping dome (Fig. 3a). The Yangliuping and Zhengziyanwuo intrusions are two economically important bodies, both of which are nearly 2000 m long and ~300 m thick. The mineralized intrusions are intensively altered to serpentinite, talc schist, tremolite schist and altered gabbro (Song et al., 2003) (Fig. 3b).

There are both disseminated and massive sulfide ores in the Yangliuping and Zhengziyanwuo intrusions. Disseminated ores are hosted only in serpentinite and account for more than 95% of Ni, Cu, Co and PGEs reserves of the two intrusions. Densely disseminated ores in the two intrusions contain ~20 to > 30 vol% sulfides, whereas weakly mineralized ores have < 10 vol% sulfides, are usually located above the densely disseminated ores. Massive ores that contain 85–95 vol% sulfides occur at the bottom of the intrusions or within the immediate footwall. Sparse network ores at the margins of the orebodies

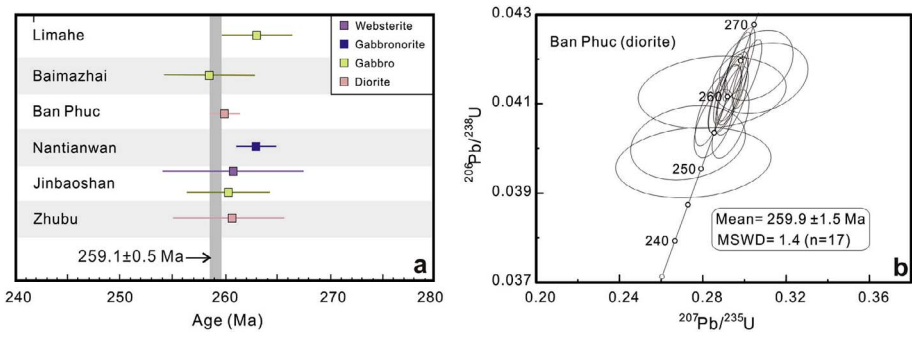

Fig. 2. (a) Compilation of available zircon U-Pb ages for Ni-Cu-(PGE) sulfide-bearing, mafic-ultramafic intrusions in the Emeishan LIP. Data sources: Baimazhai No.3 intrusion from Wang et al. (2006); Limahe and Zhubu from Zhou et al. (2008); Nantianwan from Wang et al. (2012a); Jinbaoshan from Tao et al. (2009); Ban Phuc, this study. Note that 259.1 ± 0.5 Ma is referred to as the termination age of the Emeishan flood basalts (Zhong et al., 2014); (b) Concordia plots of U-Pb isotopic compositions for zircon grains from a diorite sample of the Ban Phuc intrusion.

Table 2
SHRIMP zircon U-Pb ages for the zircon from a diorite sample of the Ban Phuc intrusion in northern Vietnam.

Spot	$^{206}Pb_c$ (%)	U (ppm)	Th (ppm)	$^{232}Th/^{238}U$	$^{206}Pb^*$ (ppm)	$^{207}Pb^*/^{206}Pb^*$	%	$^{207}Pb^*/^{235}U$	%	$^{206}Pb^*/^{238}U$	%	$^{206}Pb/^{238}U$ Age (Ma)
BP-1-1	0.01	2222	942	0.44	79	0.05160	1.1	0.29,440	1.7	0.04139	1.2	261.4 ± 3.2
BP-1-2	0.00	2705	1364	0.52	96	0.05164	1.2	0.29,400	1.7	0.04129	1.2	260.8 ± 3.1
BP-1-3	2.36	685	225	0.34	24	0.04930	6.5	0.27,300	6.7	0.04013	1.4	253.6 ± 3.4
BP-1-4	0.06	2072	886	0.44	73	0.05133	1.3	0.29,080	1.8	0.04109	1.2	259.6 ± 3.1
BP-1-5	0.38	4038	2247	0.57	146	0.05152	1.1	0.29,780	1.6	0.04193	1.2	264.8 ± 3.2
BP-1-6	0.56	1949	546	0.29	68	0.05103	1.8	0.28,530	2.2	0.04056	1.2	256.3 ± 3.1
BP-1-7	–	1534	612	0.41	55	0.05129	1.0	0.29,230	1.6	0.04133	1.3	261.1 ± 3.2
BP-1-8	0.34	2800	1360	0.50	99	0.05191	1.3	0.29,390	1.8	0.04107	1.2	259.4 ± 3.1
BP-1-9	0.19	3233	1536	0.49	116	0.05243	1.0	0.30,120	1.6	0.04166	1.2	263.1 ± 3.2
BP-1-10	0.24	2159	1121	0.54	76	0.05123	1.3	0.29,040	1.8	0.04111	1.2	259.7 ± 3.2
BP-1-11	0.11	1813	661	0.38	64	0.05045	1.3	0.28,400	1.8	0.04083	1.2	258.0 ± 3.2
BP-1-12	3.56	2602	1195	0.47	96	0.05370	4.7	0.30,800	4.9	0.04157	1.3	262.6 ± 3.2
BP-1-13	0.02	3020	1756	0.60	109	0.05137	0.8	0.29,630	1.5	0.04183	1.2	264.2 ± 3.2
BP-1-14	0.34	1858	602	0.33	65	0.05246	1.6	0.29,330	2.0	0.04055	1.2	256.2 ± 3.1
BP-1-15	7.00	3309	1769	0.55	121	0.05030	8.8	0.27,500	8.9	0.03968	1.3	250.9 ± 3.2
BP-1-16	3.12	3903	2786	0.74	145	0.05300	3.6	0.30,600	3.8	0.04186	1.2	264.4 ± 3.2
BP-1-17	4.45	1997	324	0.17	74	0.05000	8.1	0.28,500	8.2	0.04126	1.3	260.6 ± 3.3

Errors are 1-sigma; Pb_c and Pb* indicate the common and radiogenic portions, respectively. Common Pb corrected using measured ^{204}Pb.

contain < 20 vol% sulfides. In addition, sulfide veinlets which occur along fractures in the intrusions and intermittently within the sills generally strike ENE (Song et al., 2003).

3.1.2. Qingkuangshan intrusion

The Qingkuangshan intrusion is located in the southern part of the Huili region, Guizhou Province (Figs. 1 and 4) and has been described by Zhu et al. (2011, 2012). There are numerous Proterozoic to Permian, mafic-ultramafic intrusions in this region (Fig. 4a). More than 20 Permian intrusions host Ni-Cu-(PGE) sulfide mineralization, however, only the Limahe and Qingkuangshan intrusions host economically important deposits. The Yanghewu and Hetaoshu intrusions are only weakly mineralized and many others are nearly barren (Fig. 4a).

The Qingkuangshan intrusion is controlled by the Hekou duplex anticline and the Anninghe-Yimen deep fault. The core of the Hekou anticline is composed of the Mesoproterozoic Hekou Group, which, from the base upward, is composed of garnet-mica schist, mica schist with quartz hornfels, mica schist with dolomitic marble, siliceous slate, quartzite and black, carbonaceous phyllite (Zhu et al., 2011). The Qingkuangshan intrusion intrudes the Hekou Group along a NS-striking fault so that the intrusion is a dyke-like body about 200 m long and 20–50 m wide and has a funnel shape extending for about 150–180 m vertically in cross section (Fig. 4b and c).

The intrusion is composed of peridotite, wehrlite and gabbro from the center to both sides and a major ore body is hosted in peridotite and wehrlite at the base of the intrusion (Fig. 4b and c). The ultramafic rocks of the intrusion have been partially altered but a poikilitic texture is still preserved. The ore body is concordant with the intrusion in shape and is cut by a NE-striking fault at depth, offsetting the uneconomic mineralization (Zhu et al., 2011).

The ore body is mostly composed of disseminated ores, which are typically hosted in peridotite. Sparsely disseminated ores are commonly underlain by densely disseminated ores. Minor amounts of massive ore either form sac-like bodies controlled by faults and fractures, or occur in the central part of densely disseminated ores (Zhu et al., 2011). The deposit has been mined out, and samples were not available for Ni, Cu and PGE analyses.

3.2. Ni-Cu sulfide-dominated intrusions

3.2.1. Limahe intrusion

The geology of the Limahe intrusion (Figs. 1 and 4a) in the northern part of the Huili region has been described by Zhou et al. (2008) and Tao et al. (2008). This body intrudes the Proterozoic pyrite-bearing quartzite, graphitic slate and siliceous limestone of the Huili Group, and is exposed over an area about 900 m long and 180 m wide. The vertical downward extension of the intrusion exceeds 200 m.

The intrusion is lopolithic in shape and divided into two lithologic units (Tao et al., 2008); a mafic unit to the east and an ultramafic unit to the west divide by a sharp contact and an abrupt change in mineral modal compositions (Fig. 5a). The mafic unit comprises a diorite zone at the top and a gabbro zone at the bottom with a transitional contact, whereas the ultramafic unit consists of wehrlite and olivine websterite also with a gradational contact between them (Fig. 5b). The ultramafic unit constitutes about one third of the total volume of the intrusion, and in many locations, is in fault contact with the country rocks. The igneous rocks are partially altered; olivine in the ultramafic rocks is partially altered to serpentine, pyroxenes in both the ultramafic and mafic rocks are partially altered to chlorite and tremolite, and plagioclase in the mafic rocks is partially altered to sericite, epidote and albite

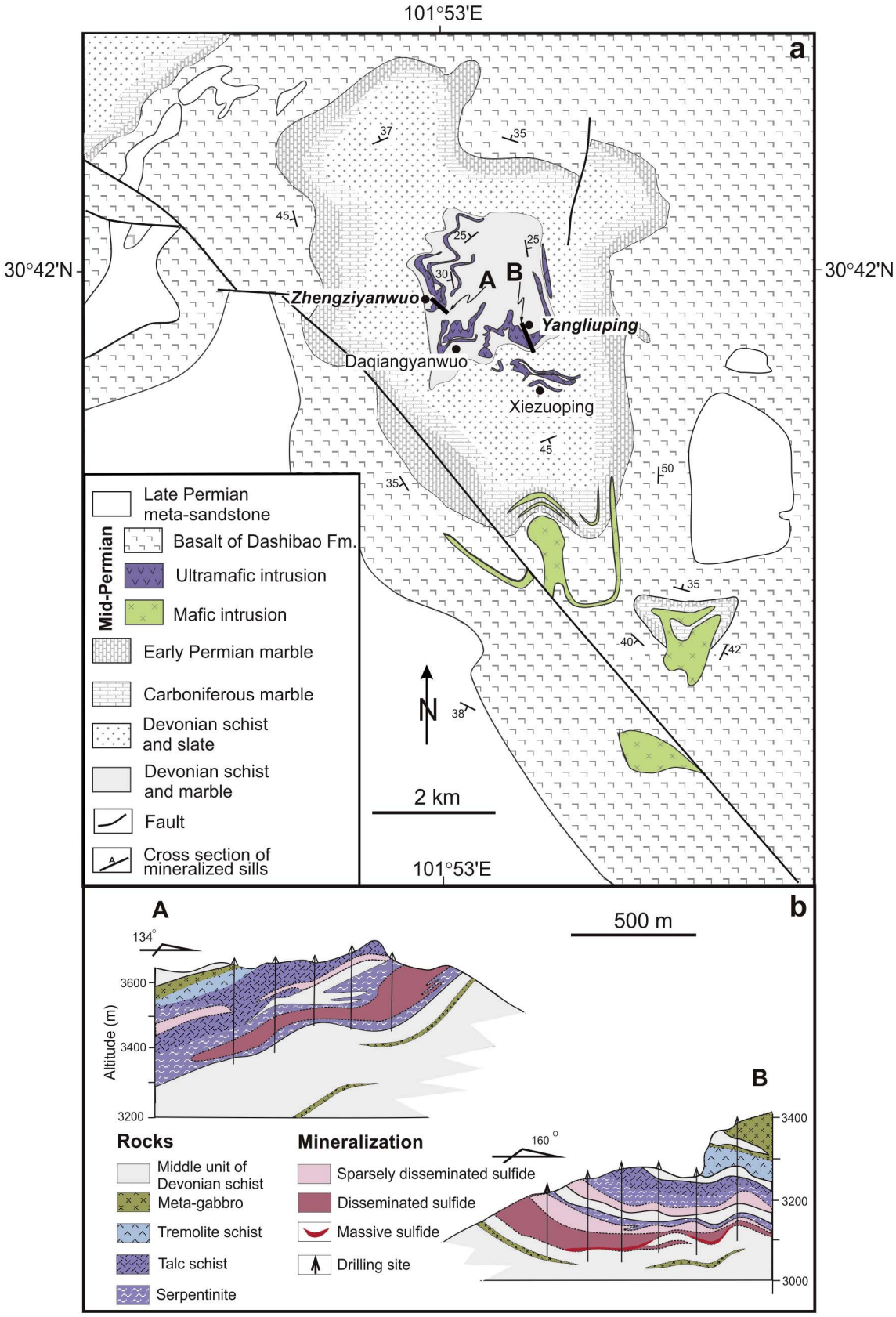

Fig. 3. Geological map of the Danba region in Sichuan Province, SW China, showing the distribution of the mafic-ultramafic intrusions including the Yangliuping, Zhengziyanwuo, Xiezuoping and Daqiangyanwuo, Dahaizi and Yuhaizi (a), and two exploration cross-sections of the Yangliuping and Zhengziyanwuo intrusions (b) (modified after Song et al., 2003).

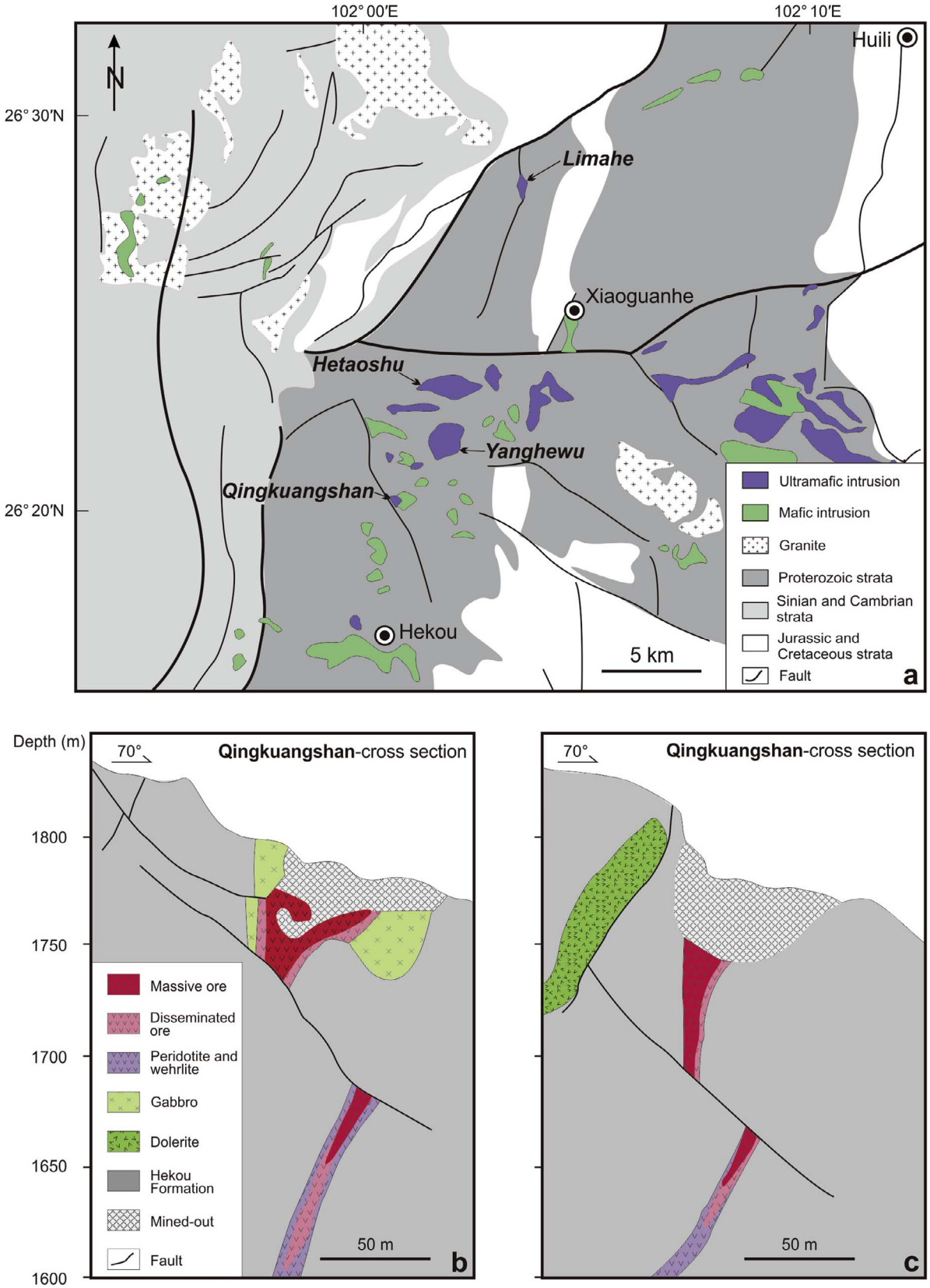

Fig. 4. Geological map of the Huili region in Guizhou Province, SW China, showing the distribution of mafic-ultramafic intrusions (a), and two cross-sections of the Qingkuangshan intrusion (b and c) (after Zhu et al., 2012).

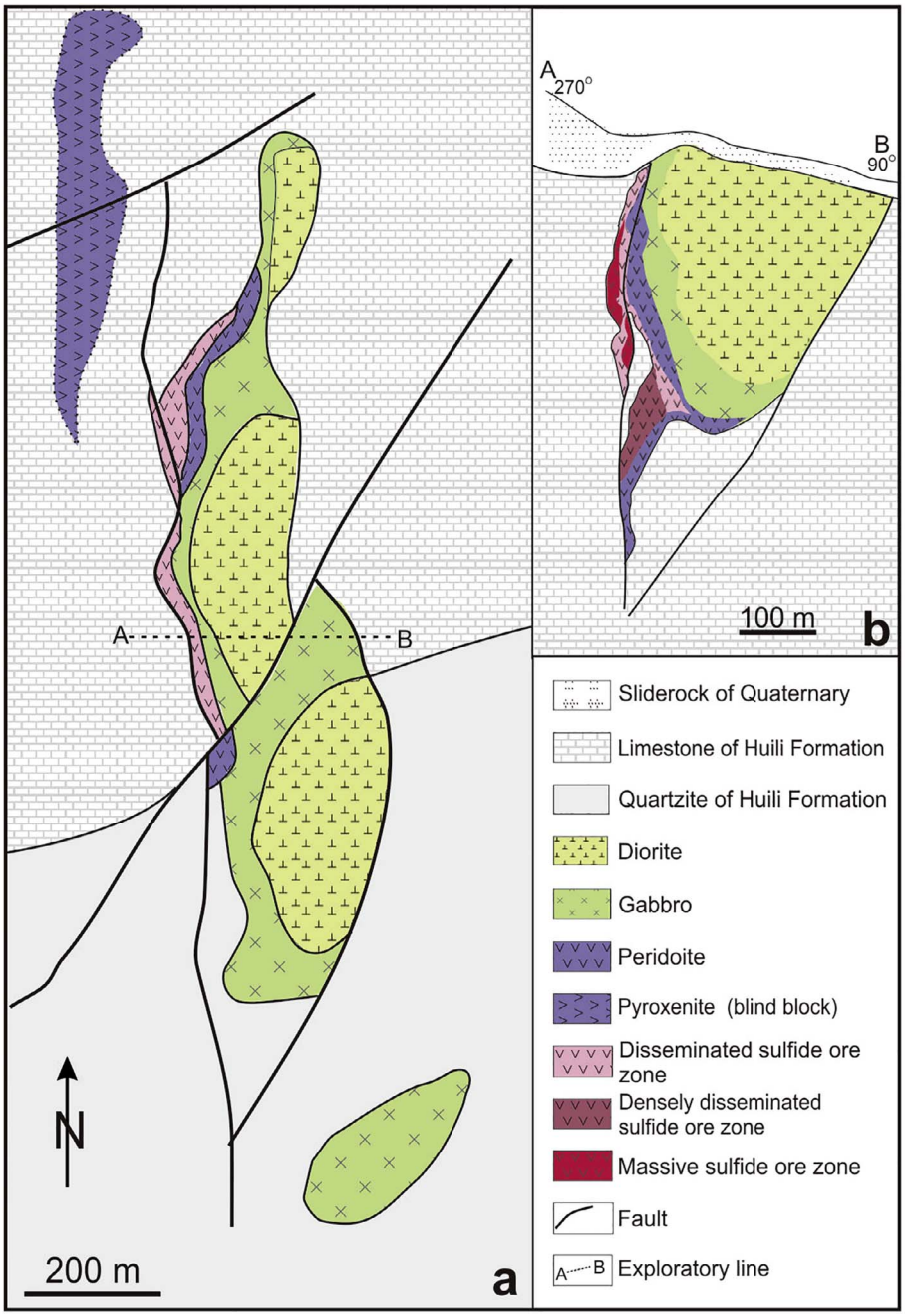

Fig. 5. Plan view (a) and cross-section (b) of the Limahe intrusion in the Huili region, Guizhou Province, SW China (after Tao et al., 2008).

(Tao et al., 2008).

Sulfide mineralization is only observed in wehrlite and olivine websterite. Rocks of the ultramafic unit commonly contain disseminated or net-textured ore, whereas massive ores mainly occur as concordant lenses within the ultramafic unit. The overall orientations of massive and net-textured sulfide zones are subparallel to layering in the mafic unit. Several massive sulfide lenses occur along contacts with the sedimentary country rocks. The total ore resource is less than 3 Mt and the average grades of the ores are ~1 wt% Ni and ~0.6 wt% Cu (Zhang and Wang, 1996).

3.2.2. *Baimazhai No.3 intrusion*

The Baimazhai No.3 intrusion is located in the Jinping region, Yunnan Province, where the flood basalts lie south of the Ailao Shan-Red River (ASRR) fault zone (Fig. 1). The flood basalts in Jinping, up to 4.5 km thick, lie between the early Permian Yangxin Formation and the Triassic Gejiu Formation (Xiao et al., 2003). The basaltic sequence consists mainly of massive, aphyric or weakly plagioclase-phyric lavas with small amounts of interlayered volcanic breccia and tuff. In the Baimazhai-Santaipo area northwest of Jinping, a group of small, differentiated plutonic bodies associated with the Emeishan flood basalts intrude the Ordovician meta-sandstone and slate. One of these, the Baimazhai No.3 intrusion, hosts a Ni-Cu sulfide-dominated deposit (Fig. 6a) (Wang et al., 2006; Wang and Zhou, 2006; Sun et al., 2008). The intrusion is lens-shaped, about 530 m long, 190 m wide and 24 to 64 m thick; it trends 296° and plunges 22°NE. The intrusion crops out over an area of 0.1 km^2, and its major part lies below the surface (Wang et al., 2006). The intrusion itself is cut by the Cenozoic lamprophyre dykes (Guan et al., 2003).

Major rock types include orthopyroxenite, websterite and gabbro, which form a concentric body with an inner core of orthopyroxenite surrounded by websterite, which in turn, is rimmed by gabbro (Fig. 6b). The massive ore body in the central part of the intrusion is about 425 m long, 40–72 m wide, and 0.7–21 m thick. The proportion of gabbro,

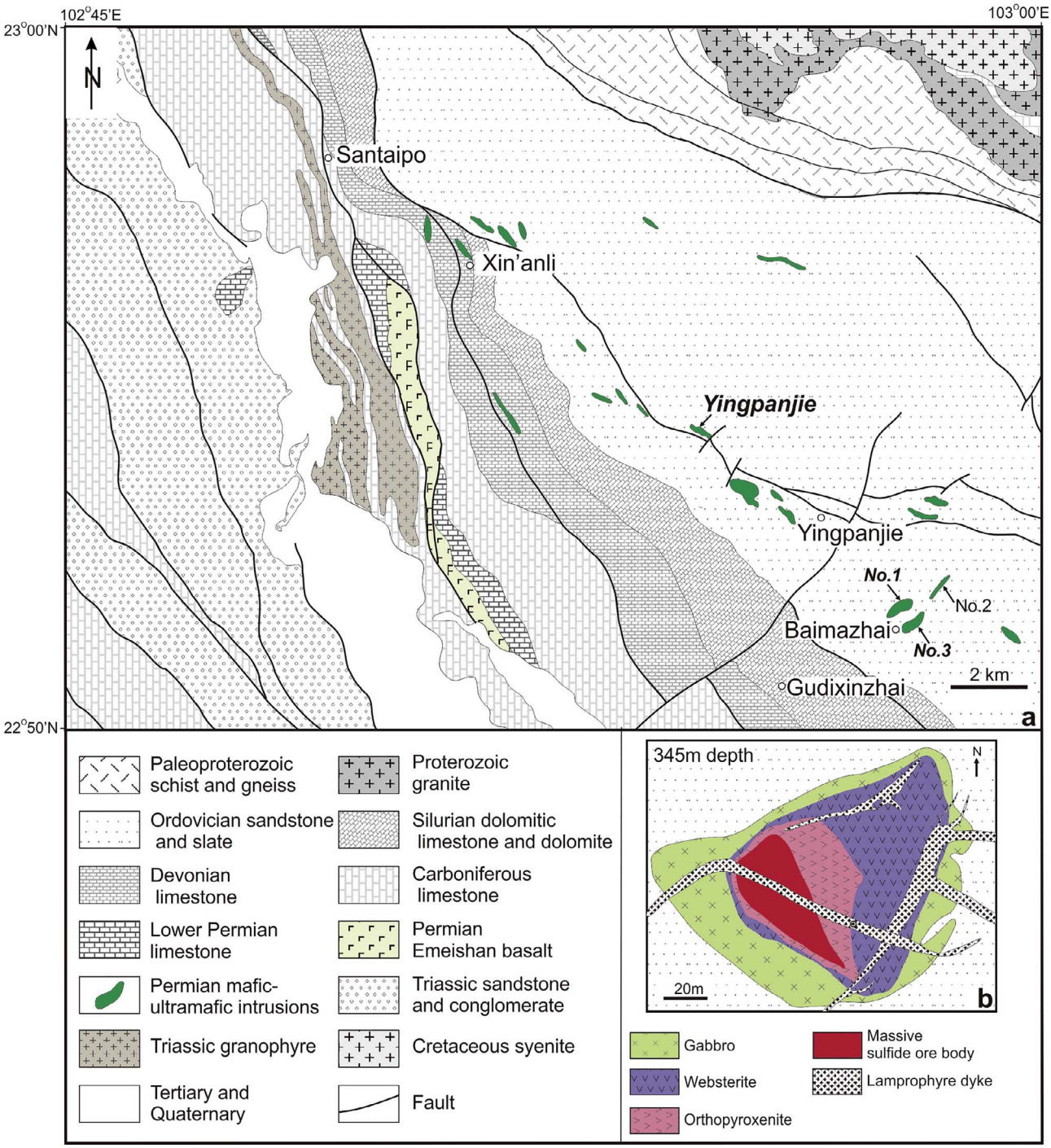

Fig. 6. (a) Simplified geological map showing the distribution of the Permian Emeishan flood basalts and mafic–ultramafic intrusions in the Baimazhai-Santaipo area, Jinping region in Yunnan Province, SW China (after Wang and Zhou, 2006), and (b) a plan view of the Baimazhai deposit at 345 m depth (after Wang et al., 2006).

websterite, orthopyroxenite and massive ore in the intrusion is approximately 30, 30, 20 and 20 vol%, respectively. Extensive alteration of the rocks resulted in the replacement of orthopyroxene by cummingtonite, clinopyroxene by tremolite, and plagioclase by albite, although relict hypersthene can be still observed in some phenocrysts (Wang et al., 2006).

Both orthopyroxenite and websterite are variably mineralized and have net-textured ore and disseminated ore, respectively. In some parts of the websterite, small sulfide aggregates are isolated by silicate minerals (Fig. 11a). The gabbro is generally sulfide-barren. The massive and net-textured ores account for about 90% of the Ni, Cu and PGE reserves of the intrusion, and they generally have sharp contacts with each other. Massive sulfide ore bodies intruded country rocks in some places (Fig. 11b). Massive ores have sulfides ranging from 52 to 88 wt% with an average of about 3.1 wt% Ni, 2.9 wt% Cu and 0.09 wt% Co. Net-textured ores contain variable amounts of sulfides ranging from 1.2 to 61 wt% with an average of 1.0 wt% Ni, 0.7 wt% Cu and 0.03 wt% Co. The total PGE contents of the massive ores range from 85 to 524 ppb, and the net-textured ores average about 60 ppb. In addition, minor brecciated ores along the margin of the intrusion locally form thin layers with thicknesses ranging from 0.8 to 5 m. The brecciated ores are composed of silicate fragments cemented by sulfides, locally associated

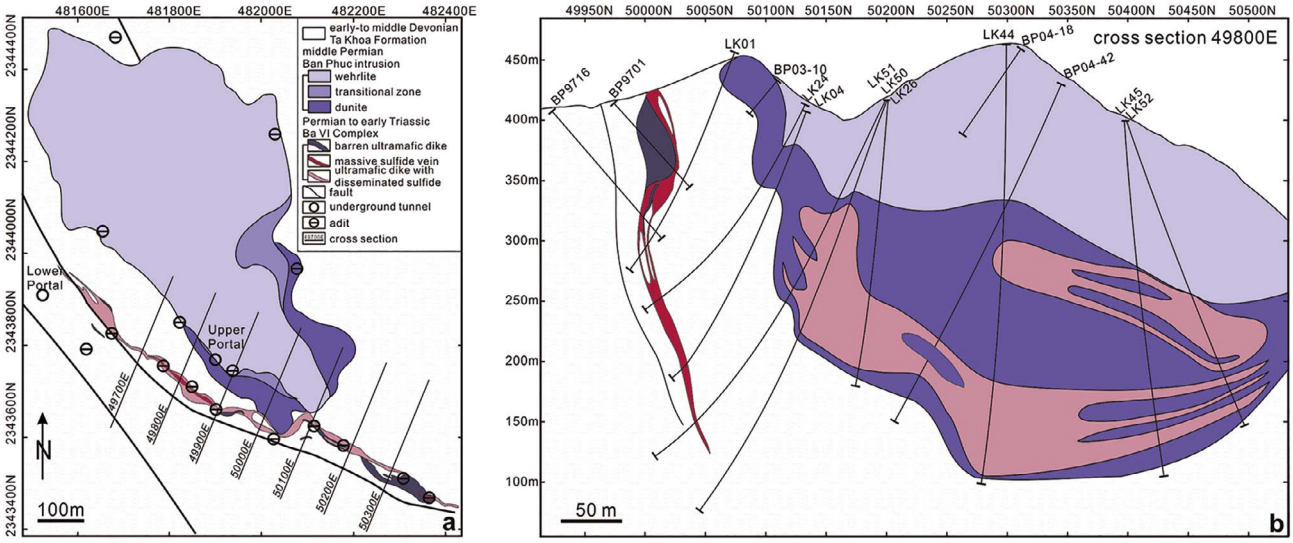

Fig. 7. Plan view (a) and cross-section (b) of the Ban Phuc intrusion in the Ta Khoa region, northern Vietnam.

with quartz and carbonate. The cementing sulfides consist of the same minerals as the massive ores but have relatively high contents of chalcopyrite (Wang and Zhou, 2006) (Fig. 11c).

3.2.3. Ban Phuc intrusion

The Ban Phuc intrusion in the northern Vietnam (Fig. 1) intrudes the core of the Ta Khoa anticline. The fold axis strikes NW and extends for ~50 km along the Song Da Rift with a width of up to 20 km (Glotov et al., 2001; Wang et al., 2007). The fold is composed of the early- to middle-Devonian schist, quartzite, gneiss, marble, siliceous limestone and amphibolite belonging to the Ta Khoa Formation in the core and is covered by the Permian lavas in the limbs. The core part of the fold experienced significant erosion and is aligned nearly vertically.

The Ban Phuc intrusion, one of the largest ultramafic bodies in the region, is a NW-trending, elongate body corresponding to the strike of the Ta Khoa Formation. It is about 940 m long and 220–420 m wide and has a 470 m downward extension, with an outcrop area of > 0.25 km^2 (Fig. 7a). It intrudes along the trend of a discontinuous unit of crystalline limestone. The intrusion is relatively wide in the northwest, and only the flat base of the intrusion is preserved. It narrows and extends to the southeast where it has an oval-like cross-section dipping steeply northeast, roughly concordant with the country rocks (Fig. 7b).

The Ban Phuc intrusion is composed of dunite overlain by wehrlite (Fig. 7b). Two main types of mineralization are recognized in the host intrusion and country rocks: (1) vein-like massive and minor disseminated ores in hornfels and altered ultramafic dykes in the southern contact zone (Fig. 7a); (2) disseminated ores at the base of the dunite unit and in the walls of the intrusion (Fig. 7b). This deposit is estimated to have significant metal reserves including 119,400 tons Ni, 40,500 tons Cu, 3400 tons Co, 14 tons Te, and 67 tons Se (Tran Van Tri, 1995; Le Van De, 1995).

One vein-like, massive ore body in the hornfels occurs along a shear-controlled vein structure in the southern margin of the intrusion (Fig. 7a and b). This ore body mainly forms a single structure with minor offshoots and bifurcations. It strikes NW with a steep dip of 70–90° to the southeast and rarely, to the southwest (Fig. 7b). Generally it cuts the lithological layering of the country rocks at a low angle but appears to be conformable in some sections (Fig. 11d). The vein is 750 m long and has an average width of 1.3 m. It has an inverted triangular form in plan view and extends downward at least 450 m (Fig. 7b). The average grade of the massive ore in the vein is 2.7% Ni, 1.2% Cu and 0.06% Co. Massive ores that were analyzed in this study have, on average, ~4.1 wt% Ni and 0.3 wt% Cu.

Disseminated ores in hornfels and altered ultramafic dykes abutting the massive ores form a halo surrounding the massive vein (Fig. 7a and b). The halo can vary from a few centimeters to several meters in width. Disseminated ores in the vein have, on average, 0.7% Ni, 0.6% Cu and 0.02% Co.

Disseminated ores in the dunite unit form concave layering which is defined by low-grade, Ni-rich sulfide layers, conformable with the base and foot walls of the intrusion (Fig. 7b). In the wider basal zone preserved at the northwestern margin of the intrusion these are flat layers with only minor convexity, but in the southeastern section the layers are tightly packed and strongly concave, extending into the footwall wall of the intrusion. Disseminated ore bodies have thicknesses varying from 2 to 40 m with an average of 0.8% Ni.

3.2.4. Nantianwan intrusion

The Nantianwan intrusion is located in the Panxi region, Sichuan Province (Fig. 1) and was described by Wang et al. (2012a,b) and Zhang et al. (2017). The intrusion is about 14 km long, 600 m to 4.5 km wide and extends downward for 100–400 m. It is hosted in the Sinian strata composed of clastic sedimentary rocks and dolomite, whereas the smaller intrusions in the area intruded Sinian, Ordovician, Devonian, or Permian strata (Fig. 8a).

Drill cores reveal that the Nantianwan intrusion consists of a gabbronorite unit, an olivine gabbro unit, and a transitional zone between them. The olivine gabbro is in contact with footwall rocks of the Sinian strata (Fig. 8). In plan view, this unit appears to intrude the gabbronorite (Fig. 8a), however, in cross-section, the olivine gabbro occurs at the bottom and is overlain by the transitional zone and then by the gabbronorite (Fig. 8b).

The olivine gabbro is composed of 30–60 modal% olivine, 15–30% plagioclase, 5–20% orthopyroxene, 5–15% clinopyroxene, < 2% chromite and < 1% sulfide and has a poikilitic texture. It contains 0.2–0.9 wt% sulfide and highly variable PGE (17–151 ppb). The gabbronorite has an ophitic texture and is composed of 40–55 modal % plagioclase, 20–35% clinopyroxene, < 25% orthopyroxene, < 10% olivine, < 3% Fe-Ti oxide and < 5% sulfide. Sulfide-bearing gabbronorites contain 1.9–4.1 wt% sulfide and 37–160 ppb PGE. Sulfide-poor gabbronorites have 0.1–0.6 wt% sulfide and 0.2–15 ppb PGE (Wang et al., 2012a).

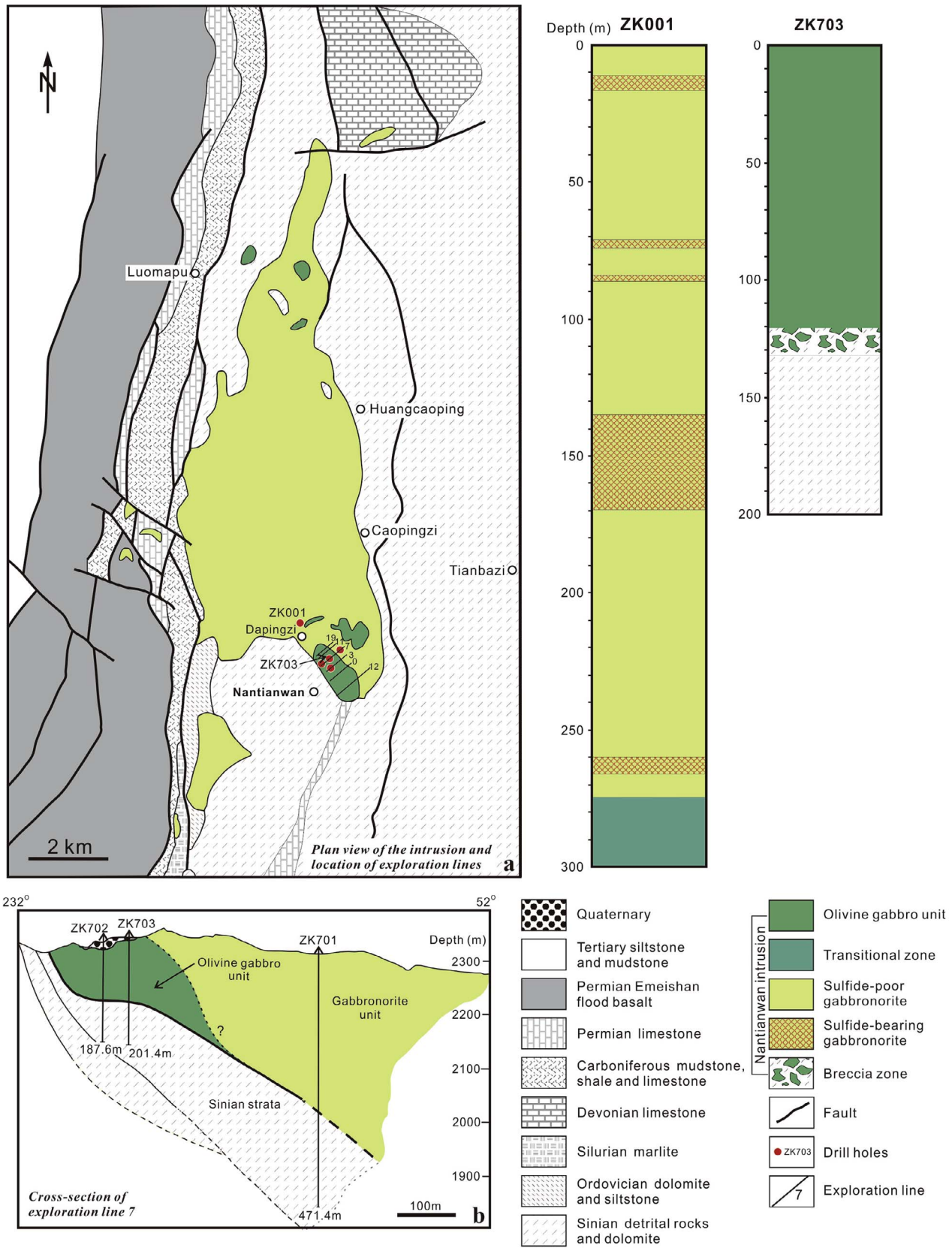

Fig. 8. Plan view of the Nantianwan mafic intrusion in the Panxi region, Sichuan Province, SW China (a) and a cross-section of exploration line 7 (b). Two columns of drill holes ZK001 and ZK703 show the distribution of three rock units of the Nantianwan intrusion (after Wang et al., 2012a).

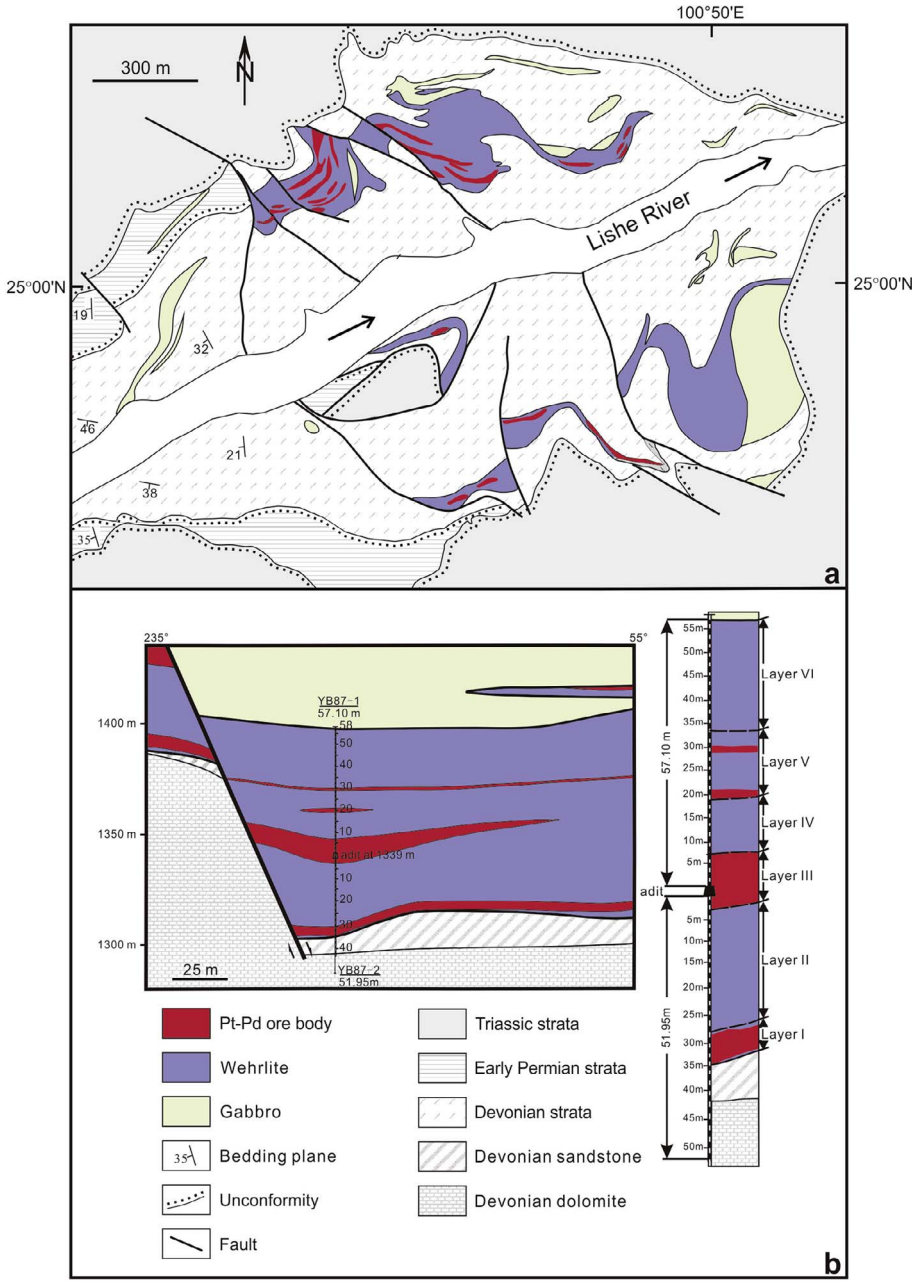

Fig. 9. (a) Simplified geological map showing the distribution of the Jinbaoshan mafic-ultramafic intrusions and ore bodies in the Midou region, Yunnan Province, SW China, and (b) cross-section of the Jinbaoshan intrusion along exploration line 315 N2 and columns of drill holes YB87-1 and YB87-2 showing the distribution of rock units (after Wang et al., 2010).

3.3. PGE-dominated intrusions

3.3.1. Jinbaoshan intrusion

The Jinbaoshan intrusion is located in the Midou region, Yunnan Province (Fig. 1), and has been described by Wang et al. (2005, 2008) and Tao et al. (2007). In this region, there are 21 mafic and 11 ultramafic sills intruding the Devonian and lower Permian strata. The ultramafic sills have intrusive relationships with associated mafic sills (Fig. 9a). The Devonian strata consist of inter-layered dolomite, sandstone and slate, whereas the lower Permian strata are limestone and sandy slate. The Devonian and Permian strata form an anticline-like dome, which is separated from Triassic strata by an unconformity and cut steeply by the Lishe River (the upstream of the Red River) (Fig. 9a).

The Jinbaoshan intrusion is about 4760 m long, 760–1240 m wide and 8–170 m thick, being the largest ultramafic sill in the area. It contains three, major, PGE-rich layers, which are defined as rocks having > 0.5 ppm Pt + Pd. Boundaries between the PGE-rich layers and the host rocks are transitional. The largest PGE-rich layer at the base of the sill is about 2100 m long, 400–600 m wide and 4–16 m thick and accounts for 44% of the total ore reserve (Wang et al., 2005). Two relatively small PGE-rich layers are located in the middle to upper parts of the sill. A chromite-rich layer, several tens of centimeters thick, which occurs discontinuously at the base of the sill, contains less than 20 vol% chromite (Wang et al., 2010). In cross section, the sill can be divided into six layers based on Pt and Pd concentrations of the rocks; three PGE-rich layers (Layers I, III and V) are interlayered with three PGE-poor layers (Layers II, IV and VI) (Fig. 9b).

The Jinbaoshan intrusion is composed mainly of wehrlite with minor olivine clinopyroxenite and clinopyroxenite. The PGE-rich layers have granular to poikilitic textures and display a primary silicate mineral assemblage consisting chiefly of olivine and clinopyroxene, similar to that of the PGE-poor layers.

3.3.2. Zhubu intrusion

The Zhubu intrusion is located in the Yuanmou region, Yunnan Province (Fig. 1), and was described in Zhu et al. (2007) and Tang et al.

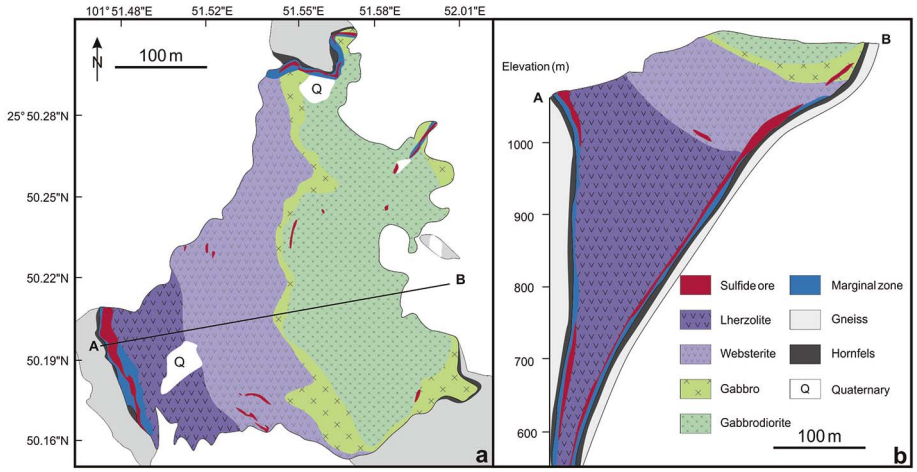

Fig. 10. Simplified geological map (a) and cross-section (b) of the Zhubu mafic-ultramafic intrusion in the Yuanmou region, Yunnan Province, SW China (after Tang et al., 2013).

(2013). The intrusion covers an area ~750 m long and ~400 m wide. The downward extension of the intrusion exceeds 580 m (Tang et al., 2013).

The Zhubu intrusion is composed of a layered sequence and a marginal zone that wraps around the layered sequence (Fig. 10a). The layered sequence represents > 90 vol% of the intrusion and is characterized by sub-horizontal modal layering with gradational contacts. It is composed of lherzolite and olivine websterite at the bottom and gabbro and gabbrodiorite at the top (Fig. 10b) (Tang et al., 2013).

The marginal zone is discordant with the layered sequence and is ~10–40 m across. It is composed of lherzolite, olivine websterite, websterite and gabbro. Small gneissic inclusions (< 10 cm in diameter) are present in places in the gabbro. No chilled rocks are present between the marginal zone and the layered sequence. A 0.5- to 1-m-thick zone of hornfels is present between the marginal zone and the Precambrian gneissic country rocks (Tang et al., 2013).

The major disseminated sulfide ores occur in the marginal zone, which is characterized by irregular metal variations. Small lenses of disseminated sulfides are also present within the layered sequence, but they are volumetrically insignificant. Nickel and Cu grades are up to 0.8 wt%, whereas Pt and Pd grades are up to 3 ppm (Tang et al., 2013).

4. Whole-rock and mineral isotopic compositions

4.1. Whole-rock Re-Os and Sm-Nd isotopic compositions

Only rocks from the Limahe and Jinbaoshan intrusions were previously analyzed for both Re-Os and Sm-Nd isotopic compositions (Tao et al., 2007, 2008). In this study, we obtained whole-rock Re-Os and Sm-Nd isotopic compositions of the rocks from the Ban Phuc intrusion and compared them with those for the high-Ti and low-Ti picrites of the Emeishan LIP and picritic dykes from the Panzhihua intrusion (Fig. 12 and Table 3).

Rocks from the Limahe, Ban Phuc and Jinbaoshan intrusions overall have highly variable εNd(t) and γOs(t) with εNd(t) ranging from −9.5 to +0.8 and γOs(t) from +5.4 to +77. These values are in sharp contrast to the relatively restricted εNd(t) and γOs(t) for both the high-Ti and low-Ti picrites of the Emeishan LIP (Fig. 12). The low-Ti picrites in the Na Muoi River region, northern Vietnam, have high and positive εNd(t) of +3.2 to +8.0 and mantle-like, restricted γOs(t) of −0.3 to

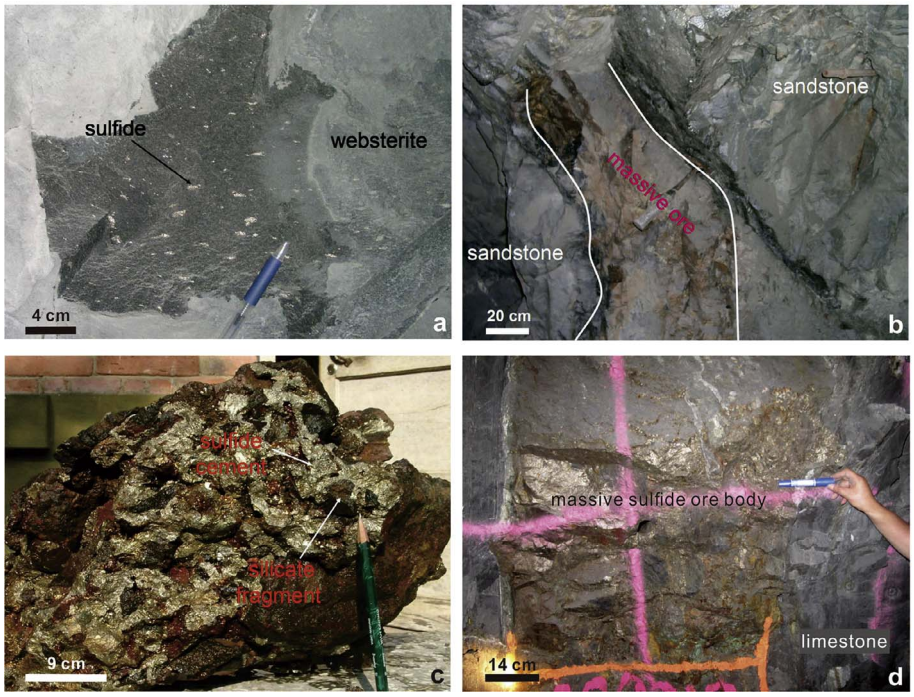

Fig. 11. Outcrops of sulfide ores of the Baimazhai No.3 and Ban Phuc intrusions. (a) Massive ore body of the Baimazhai No.3 intrusion intruded into the country rocks of the Ordovician sandstones at 315 m depth; (b) sulfide aggregates disseminated in the websterite of the Baimazhai No. 3 intrusion; (c) brecciated ore of the Baimazhai No.3 intrusion showing silicate fragments cemented by sulfides, and (d) sulfide ore body of the Ban Phuc intrusion cuts lithological layering of the country rocks at a low angle but appears conformable in some sections.

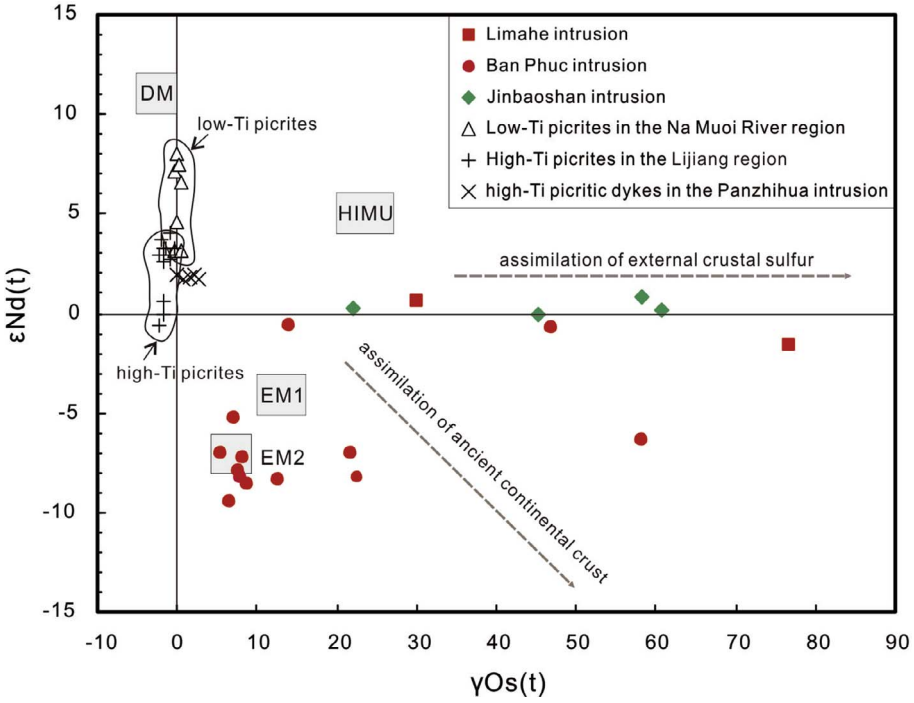

Fig. 12. Plot of εNd(t) versus γOs(t) values for picrites and the rocks from the Ni-Cu-(PGE)-sulfide-bearing mafic-ultramafic intrusions in the Emeishan LIP. Data sources: Limahe from Tao et al. (2008); Ban Phuc, this study; Jinbaoshan from Tao et al. (2007); low-Ti picrite from Hanski et al. (2004); high-Ti picrite from Zhang et al. (2008); Panzhihua picritic dyke from Hou et al. (2013). Reservoir end members of the mantle were estimated for Nd from Zindler and Hart (1986) and for Os from Shirey and Walker (1998).

+0.6, which are interpreted to have formed by high degrees of partial melting of a strongly depleted mantle source at relatively shallow depths (Wang et al., 2007).

The high-Ti picrites in the Lijiang region of SW China have εNd(t) ranging from −0.6 to +4.0 and restricted γOs(t) of −2.4 to −0.8 (Zhang et al., 2008). The low γOs(t) of the high-Ti picrites is considered to be unusual in terms of plume-related origin and indicate there were no recycled crustal components in the mantle source or no significant interaction of picrites with ancient subcontinental lithospheric mantle of the Yangtze Block (Zhang et al., 2008). Rocks of the Abulangdang intrusion in the Panxi region have γOs(t) from +0.1 to +1.2 and εNd(t) values −1.9 to +2.9, similar to those of the high-Ti picrites, high-Ti flood basalts and Fe–Ti oxide-bearing, gabbroic intrusions of the Emeishan LIP (Wang et al., 2014). These rocks are considered to be cumulates of high-Ti picritic magmas and resemble the ultramafic portions that may have been lost from Fe-Ti oxide-bearing gabbroic intrusions in the Panxi region. The picritic dykes in the Panzhihua intrusion are thought to characterize the mantle source of Fe-Ti oxide-bearing, layered intrusions in the Panxi region (Hou et al., 2013). They have εNd(t) of +1.7 to +1.9 and γOs(t) of −0.1 to +2.8 (Hou et al., 2013), similar to those of the high-Ti picrites in the Lijiang region (Fig. 12). The Nd-Os isotopic compositions of the picritic dykes are attributed to the interaction of partial melts of an upwelling mantle plume with an eclogite or pyroxenite component in the lithospheric mantle (Hou et al., 2013). However, the major element compositions of the picritic dykes are thought to reflect assimilation of brucite marble by basaltic magmas (Tang et al., 2017).

4.2. S Isotopic compositions of sulfide minerals

We determined the S isotopic composition of our samples with *in situ* MC-ICP-MS analytical technique at the Geological Survey of Finland in Espoo, using a Nu Plasma HR multi-collector ICP-MS together with a Photon Machine Analyte G2 laser microprobe. We analyzed pyrrhotite, pentlandite, chalcopyrite and pyrite from sulfide ores and rocks of Ni-Cu-(PGE) sulfide-bearing, mafic-ultramafic intrusions and Fe-Ti oxide-bearing, layered intrusions in the Emeishan LIP. The results are listed in Table 4.

Disseminated ores occur in all three groups of mineralized intrusions, whereas massive and net-textured ores are only hosted in Ni-Cu-(PGE) and Ni-Cu sulfide-dominated intrusions (Song et al., 2004a,b, Song et al., 2008a,b; Wang and Zhou, 2006; Wang et al., 2006, 2010; Zhu et al., 2007;Tao et al., 2007, 2008; Zhu et al., 2012; Tang et al., 2013). Sulfides from sulfide ores of the same intrusion have a restricted $\delta^{34}S$ range, but sulfides from different intrusions overall have variable $\delta^{34}S$ values.

In the Ban Phuc intrusion, most pyrrhotite and chalcopyrite from massive, semi-massive and net-textured ores of the intrusion and those from sulfide veins in the country rocks have similarly negative $\delta^{34}S$ ranging from −4.1 to −3.4‰, whereas some pyrrhotite grains from mafic dykes and dunite have slightly low $\delta^{34}S$ of −6.7 to −5.4‰ (Table 4 and Fig. 13a). Pyrrhotite, pentlandite, chalcopyrite and pyrite from net-textured and disseminated ores of the Baimazhai No.3 intrusion have overall positive $\delta^{34}S$ ranging from +4.2 to +11.2‰, whereas pyrrhotite, pentlandite and pyrite from disseminated ores of the weakly mineralized Yingpanjie intrusion have distinctly different $\delta^{34}S$ of −0.2 to +1.5‰ (Table 4 and Fig. 13a). Chalcopyrite and pyrite in PGE-rich ores from wehrlite of the Jinbaoshan intrusion have $\delta^{34}S$ ranging from +4.1 to +6.8‰, similar to those for sulfides from the Baimazhai No.3 intrusion (Fig. 13a).

Pyrrhotite and pentlandite from olivine gabbro of the Nantianwan intrusion have highly variable $\delta^{34}S$ of +4.8 to +21.4‰, whereas pyrrhotite, pentlandite and chalcopyrite from gabbronorite have restricted $\delta^{34}S$ values of +0.8 to +3.4‰ (Table 4 and Fig. 13b).

Pyrrhotite and pyrite from gabbro of the Panzhihua, Hongge, Taihe and Baima layered intrusions have generally consistent $\delta^{34}S$ values close to that of the mantle (−0.5 ± 1‰, Labidi et al., 2013). Sulfides from gabbro of the Panzhihua, Baima and Taihe intrusions have $\delta^{34}S$ ranging from −0.8 to +1.5‰, whereas those from the Hongge intrusion have $\delta^{34}S$ ranging from +1.6 to +3.4‰ (Table 4 and Fig. 13c). Overall, sulfides from rocks of the Fe-Ti oxide-bearing, layered intrusions have more restricted $\delta^{34}S$ values than those from sulfide ores of the Ni-Cu-(PGE) sulfide-bearing intrusions in the Emeishan LIP.

Table 3
Whole-rock εNd(t) and γOs(t) for the rocks from Ni-Cu-(PGE) sulfide-bearing mafic-ultramafic intrusions, high-Ti and low-Ti picrites of the Emeishan LIP and picritic dykes in the Panzhihua layered intrusion.

Sample no.	Rock type	εNd(*t*)	γOs(*t*)	References
Limahe intrusion hosting Ni-Cu sulfide-dominated deposit				
LMU3	Olivine websterite	+0.6	+30	Tao et al. (2008)
LMS4	Olivine websterite	−1.6	+77	
Ban Phuc intrusion hosting Ni-Cu sulfide-dominated deposit				
BP-33	Harzburgite	−8.3	+23	This study
BP-36	Harzburgite	−7.0	+22	
BP-39	Harzburgite	−7.3	+8.2	
BP-42	Harzburgite	−5.2	+7.2	
BP-47	Harzburgite	−8.3	+8.0	
BP-52	Harzburgite	−8.4	+13	
BP-122	Harzburgite	−7.1	+5.4	
BP-128	Harzburgite	−6.4	+58	
BP-154	Lherzolite	−9.5	+6.7	
BP-160	Lherzolite	−7.9	+7.8	
BP-163	Lherzolite	−8.6	+8.8	
BP-138	Ol gabbro	−0.6	+14	
BP-140	Ol gabbro	−0.7	+47	
Jinbaoshan intrusion hosting PGE-dominated deposit				
145-3R	Wehrlite	+0.2	+22	Tao et al. (2007)
JB19	Wehrlite	+0.1	+61	
1309-2	Wehrlite	+0.8	+58	
B33	Wehrlite	−0.1	+45	
Low-Ti picrites in the Na Muoi River region				
B6887	Picrite	+4.6	−0.1	Hanski et al. (2004)
B6889	Picrite	+8.0	−0.1	
B6891	Picrite	+7.1	−0.3	
B6892	Picrite	+7.5	+0.1	
G1456	Picrite	+6.6	+0.4	
P11/86	Picrite	+3.2	−0.3	
P9/86	Picrite	+3.2	+0.6	
High-Ti picrites in the Lijiang region				
DJ03-30	Picrite	−0.6	−2.4	Zhang et al. (2008)
DJ03-39	Picrite	+2.9	−2.4	
DJ03-37	Picrite	+2.7	−1.0	
DJ03-44	Picrite	+2.6	−1.7	
DJ-31	Picrite	+4.0	−0.9	
DJ03-45	Picrite	+3.3	−0.4	
DJ03-46	Picrite	+0.6	−1.6	
DJ03-35	Picrite	+3.3	−1.7	
DJ03-35-1	Picrite	−0.1	−1.7	
DJ03-4	Picrite	+3.7	−1.9	
SM03-6	Picrite	+2.9	−0.8	
SM03-1	Picrite	+3.3	−1.4	
picritic dyke in the Panzhihua intrusion				
PZH1003	Picritic dyke	+1.7	+0.9	Hou et al. (2013)
PZH1004	Picritic dyke	+1.9	+0.1	
PZH1005	Picritic dyke	+1.9	+2.2	
PZH1006	Picritic dyke	+1.8	+1.6	
PZH1007	Picritic dyke	+1.9	−0.1	
PZH1009	Picritic dyke	+1.7	+2.8	

5. Platinum-group minerals and chalcophile element compositions of sulfide ores

5.1. Platinum-group minerals

Platinum-group minerals (PGM) were only investigated in the Yangliuping (Song et al., 2004b), Baimazhai No.3 (Wang and Zhou, 2006), Jinbaoshan (Wang et al., 2008) and Ban Phuc intrusions (our unpublished data). These deposits have remarkably different varieties and abundances of PGM (Table 5).

PGMs in the Yangliuping intrusion mainly occur in massive sulfide ores and include three groups: (1) Pd-Sb-Bi telluride: e.g., testibiopalladite [PdTe(Sb,Te)] and michenerite [Pd(Te,Bi)]; (2) Pt and Os arsenide: sperrylite ($PtAs_2$), omeiite and ($OsAs_2$) and (3) Pd antimonide: sudburyite (PdSb) (Song et al., 2004b) (Table 5). Three of these minerals, sperrylite, testibiopalladite and michenerite, are common in the ores. In addition, PGE-bearing sulfarsenides and Pd-bearing cobaltite (CoAsS)-gersdorffite (NiAsS) solid solution, commonly occur as single crystal inclusions in pyrrhotite and, more rarely, in pentlandite (Song et al., 2004b). The PGM and Pd-bearing cobaltite–gersdorffite solid solution is interpreted to have crystallized from residual sulfide melt that was Pt- and Pd-rich at a lower temperature (< 800 °C) after the crystallization of mss from a sulfide melt (Song et al., 2004b).

PGMs are rare in the Baimazhai No.3 intrusion; only one small froodite ($PdBi_2$) grain (~10 μm) was observed within cobaltite-gersdorffite solid solution in massive ores (Wang and Zhou, 2006) (Table 5). Like the Yangliuping and Ban Phuc intrusions, cobaltite-gersdorffite solid solution is common in massive ores and is associated with aggregates of pyrrhotite, or accompanied by crystals of pentlandite and chalcopyrite, or even enclosed within chalcopyrite. Froodite is considered to be hydrothermal in origin and may have formed by interaction of hydrothermal fluids with earlier primary sulfides, such that the PGE were remobilized and re-precipitated to form the froodite (Wang and Zhou, 2006). It is not known, however, if cobaltite-gersdorffite solid solution in the massive ores of the Baimazhai No.3 intrusion is PGE-rich and if it is also a carrier of PGE, like those in the Ban Phuc intrusion.

PGMs in the Ban Phuc intrusion are mainly observed in disseminated ores, and they include sperrylite, froodite and Au-Ag electrum (Table 5). In contrast, no or few PGM are found in massive ores, which contain much higher PGE concentrations than disseminated ores. Instead, gersdorffite is commonly enclosed within pyrrhotite of massive ores and contains all six PGE (Table 5). A few sperrylite and irarsite-platarsite (IrPtAsS) grains are enclosed in gersdorffite (our unpublished data). A possible interpretation is that the presence of As in a magma may cause early removal of PGE and the formation of early arsenic-bearing PGM and PGE-bearing sulfarsenide like gersdorffite. In contrast, the absence of As leads to late interstitial formation of As-poor PGM, like those in disseminated ores (Wang et al., unpublished data).

The Jinbaoshan intrusion contains the most abundant PGMs among all the intrusions in the Emeishan LIP. More than 130 PGM grains have been identified in a major chromite-rich layer and two PGE-rich layers of the intrusion (Wang et al., 2008). The PGM are dominated by Pd and Pt phases and are commonly Te-, Sn- and As-bearing. They can be divided into nine varieties, including moncheite ($PtTe_2$), atokite (Pd_3Sn), kotulskite (PdTe), sperrylite, irarsite (IrAsS), cooperite (PtS), sudburyite (PdSb), Pt-Fe alloy and Au-Ag electrum (Wang et al., 2008) (Table 5). Moncheite and atokite are the two most common varieties. The PGM grains are believed to be secondary phases associated with pervasive hydrothermal alteration, and are likely to have formed by expulsion of PGE from solid solution in BMS with introduction of Te, Bi, Sb and As (Wang et al., 2008).

5.2. Chalcophile element compositions of sulfide ores

Sulfide ores have highly variable chalcophile element concentrations, which are related to the sulfide contents of the ores. In general, ores of Ni-Cu-(PGE) and Ni-Cu sulfide-dominated intrusions contain more than 10 vol% sulfides (Glotov et al., 2001; Song et al., 2003, 2004b; Wang and Zhou, 2006) and have low PGE concentrations relative to ores that contain less than 3 vol% sulfides in PGE-dominated intrusions (Tao et al., 2007; Wang et al., 2010, Tang et al., 2013). On the 100% sulfide basis, massive and net-textured ores of Ni-Cu-(PGE) sulfide-dominated intrusions have overall higher Ni and PGE (especially IPGE) tenors than Ni-Cu sulfide-dominated intrusions (Fig. 14a and Table 6). Ores from the Yangliuping intrusion contain particularly high PGE tenors, whereas the ores from the Baimazhai No.3 intrusion have high Pt and Pd tenors but extremely low IPGE tenors (Fig. 14a) (see Table 6).

Disseminated ores from mineralized intrusions also have distinctive PGE concentrations (Table 7). Disseminated ores of the Yangliuping and

Table 4
S isotopic compositions of sulfides in ores and rocks of Ni-Cu-(PGE) sulfide-bearing mafic-ultramafic intrusions in the Emeishan LIP.

Intrusions	*Baimazhai No.3*									
Sample No.	BMZ-82	BMZ-82	BMZ-82	BMZ-88	BMZ-88	BMZ-88	BMZ-125	BMZ-125	BMZ-125	BMZ-80
Lithology	Net-textured ore						Disseminated ore			
Minerals (grains)	Po(2)	Pn(2)	Cpy(2)	Po	Pn	Cpy(4)	Po(3)	Pn	Cpy(4)	Po(3)
$\delta^{34}S$(‰)	6.7 ± 0.1	7.1 ± 0.1	6.5 ± 0.4	6.8	7.1	6.0 ± 1.2	6.7 ± 0.2	7.4	6.5 ± 0.4	7.0 ± 0.3
Intrusions	*Baimazhai No.3*				*Ban Phuc*					
Sample No.	BMZ-80	BMZ-80	BMZ-187	BMZ-187	BP-7	BP-9	BP-10	BP-11	BP-22	BP-61
Lithology	Disseminated ore				Massive ore					
Minerals (grains)	Pn	Cpy(2)	Py(10)	Cpy(2)	Po	Po	Po	Po	Po	Cpy
$\delta^{34}S$(‰)	6.0	6.5 ± 0.4	8.6 ± 1.4	7.3 ± 0.5	−4.1	−4.1	−4.1	−4.2	−3.9	−4.2
Intrusions	*Ban Phuc*									
Sample No.	BP-73	BP-70	BP-66	BP-66	BP-25	BP-68	BP-72	BP-138	BP-102d	BP-29
Lithology	Massive ore		Semi-massive ore	Semi-massive ore	Net-textured ore			Disseminated ore	Cu-rich ore	
Minerals (grains)	Po	Po	Po	Cpy	Po	Po + silicates	Po	Po	Cpy	Po
$\delta^{34}S$(‰)	−4.1	−3.8	−4.3	−4.2	−4.2	−4.1	−3.4	−0.4	−2.6	−4.1
Intrusions	*Ban Phuc*									*Yingpanjie*
Sample No.	BP-47	BP-92	BP-17	BP-33	BP-36	BP-42	BP-39	BP-62	BP-64	YPJ-82
Lithology	Mafic dyke	Mafic dyke	Dunite					Sandstone		Disseminated ore
Minerals (grains)	Po + silicates	Po + silicates	Po + silicates	Po	Po + silicates	Po + silicates	Po	Po	Po	Po(2)
$\delta^{34}S$(‰)	−6.7	−1.4	−6.4	−5.7	−6.7	−6.5	−6.4	−4.0	−3.9	−0.2 ± 0.0
Intrusions	*Yingpanjie*							*Nantianwan*		
Sample No.	YPJ-82	YPJ-85	YPJ-85	YPJ-85	YPJ-96	YPJ-96	YPJ-100	NT-110	NT-110	NT-74
Lithology	Disseminated ore							Gabbronorite		
Minerals (grains)	Pn(2)	Po(3)	Pn	Py	Po	Py	Po(4)	Po(4)	Cpy(4)	Po(9)
$\delta^{34}S$(‰)	0.0 ± 0.2	1.1 ± 0.4	1.2	1.2	1.4	1.0	1.2 ± 0.3	1.5 ± 0.3	1.7 ± 0.5	1.8 ± 0.2
Intrusions	*Nantianwan*									*Jinbaoshan*
Sample No.	NT-74	NT-74	NT-90	NT-90	NT-90	NT-21	NT-27	NT-37	NT-37	JB-39
Lithology	Gabbronorite					Olivine gabbro				wehrlite
Minerals (grains)	Pn(2)	Cpy(4)	Po(8)	Pn(2)	Cpy(2)	Po(5)	Po(10)	Po(9)	Pn(2)	Cpy(2)
$\delta^{34}S$(‰)	2.2 ± 0.1	1.1 ± 0.3	2.3 ± 0.5	2.0 ± 0.1	1.7 ± 0.1	10.3 ± 4.6	20.4 ± 0.5	7.2 ± 2.7	6.2 ± 0.0	5.8 ± 0.7
Intrusions	*Jinbaoshan*							*Panzhihua*	*Baima*	
Sample No.	JB-39	JB-40	JB-40	JB-41	JB-41	JB-42	JB-42	LJ-1429	BM-1415	BM-1405
Lithology	Wehrlite							Gabbro	Gabbro	
Minerals	Py(2)	Cpy(2)	Py(2)	Cpy(2)	Py(4)	Cpy(2)	Py(2)	Po(6)	Po(2)	Py(4)
$\delta^{34}S$(‰)	6.7 ± 0.0	6.1 ± 0.3	6.7 ± 0.2	4.9 ± 0.7	4.4 ± 0.3	4.4 ± 0.4	4.9 ± 0.1	0.8 ± 0.4	-0.3 ± 0.7	0.0 ± 0.4
Intrusions	*Taihe*			*Hongge*						
Sample No.	TH-1554	TH-1554	TH-1578	HG-1528	HG1528	HG-1542	HG1542-2			
Lithology	Gabbro			gabbro						
Minerals	Po(2)	Py(2)	Po(2)	Po(7)	Pn	Po(6)	Py			
$\delta^{34}S$(‰)	0.9 ± 0.3	0.8 ± 0.3	0.4 ± 0.1	2.2 ± 0.6	2.2	2.8 ± 0.3	3.0			

Note: (1) The sulfides from the Ban Phuc intrusion were analyzed at Indiana University using the continuous-flow method described in Studley et al. (2002). (1) The sulfides for other intrusions were analyzed using *in situ* LA-MC-ICP-MS method in the Finland Geological Survery in Espoo. *The numbers in the bracket refers to the grained that were analyzed in the same thin section.

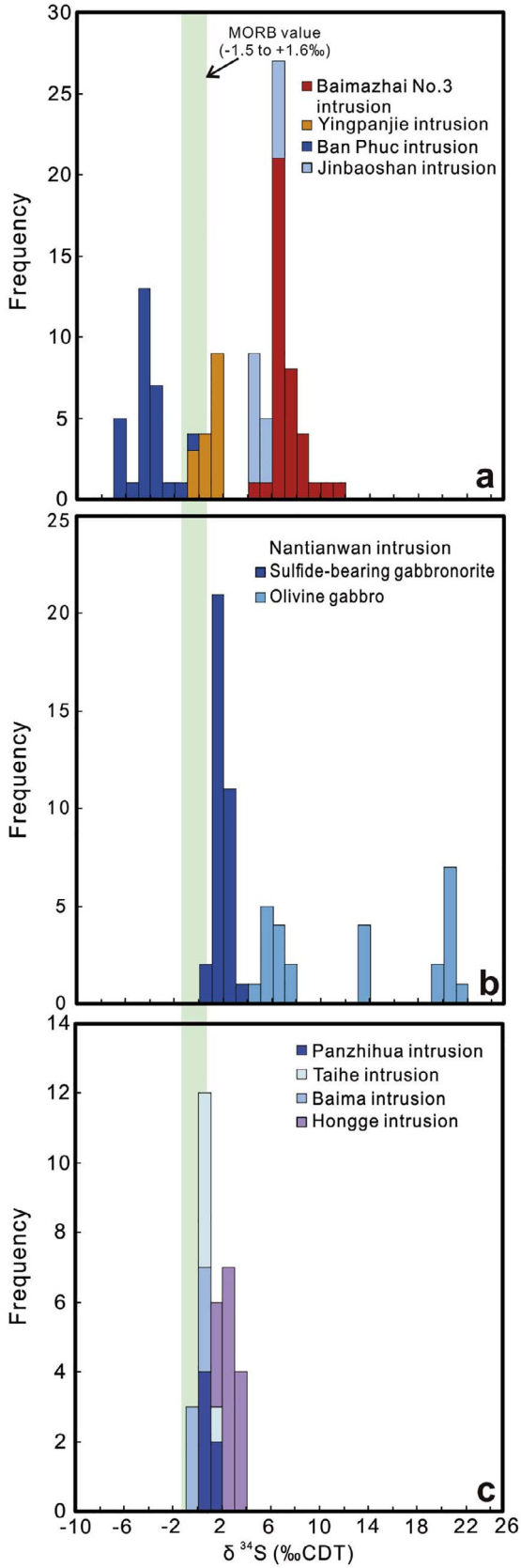

Fig. 13. Histogram of $\delta^{34}S$ for sulfides from the ores and rocks of the mafic-ultramafic intrusions in the Emeishan LIP.

Table 5
Major varieties of platinum-group minerals in the Ni-Cu-(PGE) sulfide-bearing mafic-ultramafic intrusions in the Emeishan LIP.

Intrusions	Tellurium	Stannide	Arsenide	Sulfide	Antimonide	Bismuthide	Sulfarsendide	Pt-Fe alloy	Au-Ag electum	Cobaltite-gersdorffite solid solution	References
Yangliuping	Testibiopalladite [PdTe(Sb,Te)]		Sperrylite ($PtAs_2$)		Sudburyite PdSb)			None	None	Yes	Song et al. (2004b)
Baimazhai No.3	michenerite [Pd(TeBi)]		Omeiite ($OsAs_2$)			Froodite ($PdBi_2$)				Yes	Wang and Zhou (2006)
Ban Phuc			Sperrylite ($PtAs_2$)			Froodite ($PdBi_2$)	Irrarsite (IrAsS) platarsite (IrAsS)	None	Yes	PGE-rich gersdorffite	This study
Jinbaoshan	Mmocheite ($PtTe_2$) kotulskite (PdTe)	atokite (Pd_3Sn)	Sperrylite ($PtAs_2$)	Cooperite (PtS)	Sudburyite (PdSb)		Irrarsite (IrAsS)	Yes	Yes	None	Wang et al. (2008)

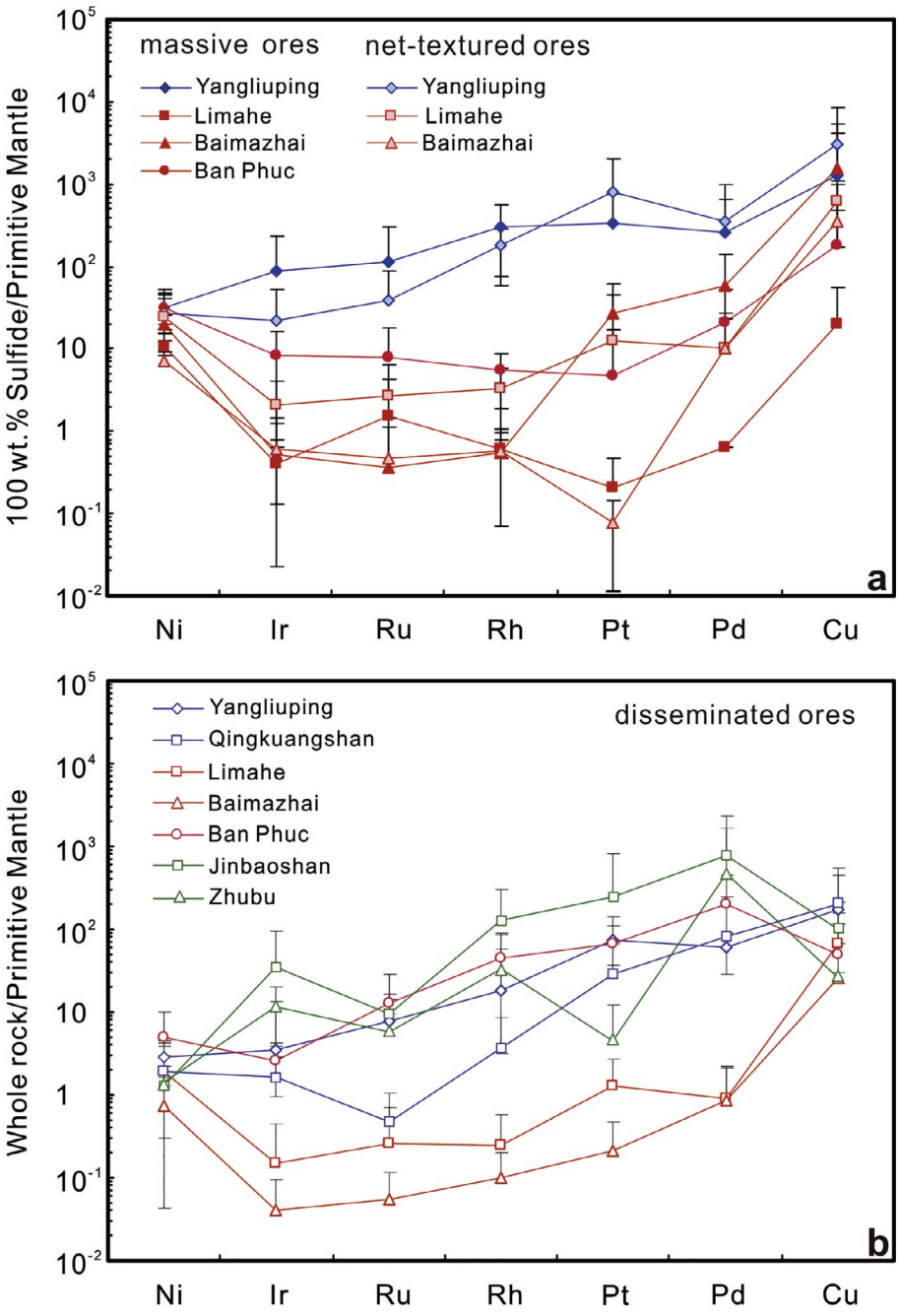

Fig. 14. (a) Primitive mantle-normalized chalcophile element patterns of massive and net-textured ores from Ni-Cu-(PGE) sulfide-bearing, mafic-ultramafic intrusions in the Emeishan LIP. Ore compositions are recalculated to 100% sulfide, and (b) Primitive mantle-normalized chalcophile element patterns of disseminated ores from Ni-Cu-(PGE) sulfide-bearing, mafic-ultramafic intrusions in the Emeishan LIP. Normalization values of the primitive mantle are from Barnes and Maier (1999) and references therein. Data sources: Yangliuping from Song et al. (2003); Qingkuangshan from Zhu et al. (2012); Limahe from Tao et al. (2008); Baimazhai No.3 from Wang et al. (2006) and Wang and Zhou (2006); Ban Phuc, this study; Jinbaoshan from Wang et al. (2010), Zhubu from Tang et al. (2013).

Qingkuangshan intrusions have much higher Ni and PGE concentrations than those from the Limahe and Baimazhai No.3 intrusions. However, disseminated ores of the Ban Phuc intrusion have Ni and PGE concentrations similar to those of the Yangliuping intrusion, which is probably because the PGEs are mainly concentrated in gersdorffite rather than sulfides (Wang et al., unpublished data). On the other hand, disseminated ores from the Jinbaoshan and Zhubu intrusions have lower Ni and much higher PGE concentrations than those from other

Table 6
Averaged Ni, Cu and PGE concentrations for massive and net-textured ores of Ni-Cu-(PGE) sulfide-bearing mafic-ultramafic intrusions in the Emeishan LIP (on the 100 wt% sulfide basis).

Intrusions	Ore types	Ni (wt.%)	Cu (wt.%)	Ir (ppb)	Ru (ppb)	Rh (ppb)	Pt (ppb)	Pd (ppb)	References
Yangliuping	Massive	6.2	3.5	306	583	295	2363	1030	Song et al. (2008b)
	Net-textured	5.3	1.4	74	191	176	5622	1438	
Limahe	Massive	2.1	0.06	1.4	7.6	0.6	1.4	2.6	Tao et al. (2008)
	Net-textured	4.9	1.8	7.2	14	3.2	90	41	
Baimazhai No.3	Massive	4.1	4.4	1.8	1.8	0.5	193	233	Wang and Zhou (2006) and Wang et al. (2006)
	Net-textured	3.3	2.5	4.5	4.7	1.2	58	100	
Ban Phuc	Massive	6.4	0.5	28	40	5.1	33	82	This study

Table 7
Averaged Ni, Cu and PGE concentrations for disseminated ores of Ni-Cu-(PGE) sulfide-bearing mafic-ultramafic intrusions in the Emeishan LIP.

Intrusions	Ni (wt.%)	Cu (wt.%)	Ir (ppb)	Ru (ppb)	Rh (ppb)	Pt (ppb)	Pd (ppb)	References
Yangliuping	0.57	0.48	12	39	18	523	240	Song et al. (2008b)
Qingkuangshan	0.37	0.55	5.56	2.40	3.52	204	329	Song et al. (2008b) and Zhu et al. (2012)
Limahe	0.39	0.19	0.52	1.28	0.23	9.10	3.62	Tao et al. (2008)
Baimazhai No.3	0.15	0.07	0.14	0.27	0.10	1.46	3.44	Wang and Zhou (2006)
Ban Phuc	0.99	0.14	9	65	42	461	812	This study
Jinbaoshan	0.25	0.28	122	47	120	1698	3075	Tao et al. (2007) and Wang et al. (2010)
Zhubu	0.18	0.07	39	29	31	2365	1890	Zhu et al. (2007) and Tang et al. (2013)

two types of intrusions (Fig. 14b).

6. Origin of magmatic Ni-Cu-(PGE) sulfide deposits in the Emeishan LIP

6.1. Nature of mantle sources

The Emeishan flood basalts were initially divided into two magma series, low-Ti and high-Ti, in terms of petrography, major and trace element and Sr-Nd isotopic compositions (Xu et al., 2001). The low-Ti series is characterized by low Ti/Y (< 500), Fe_2O_3* (< 12 wt%) and εNd(t) (−4.8 to +1.4), whereas the high-Ti series has higher TiO_2 (> 3 wt%) at a comparable Mg# and is characterized by high Ti/Y (> 500), Fe_2O_3* (12.7–16.4 wt%) and εNd(t) (+1.1 to +4.8) (Xu et al., 2001). The high-Ti and low-Ti picrites have distinctly different εNd(t) values but similar γOs(t) values (Fig. 12), which is consistent with the hypothesis that the high-Ti and low-Ti magma series were likely derived from different mantle sources that experienced different degrees of partial melting (e.g., Xu et al., 2001).

The heterogeneity of mantle sources for the Emeishan LIP has been discussed in a number of studies on the Emeishan flood basalts and mafic-ultramafic intrusions. Previous studies on typical sections of the Emeishan flood basalts and mafic-ultramafic intrusions in the Binchuan, Ertan, Longzhoushan, Funing, Dongchuan, Jinping and Song Da regions indicate that primitive magmas of the low-Ti series were likely generated by relatively high degrees of partial melting (e.g., ~16%) of a depleted mantle source around the spinel-garnet transition zone, whereas primitive magmas of the high-Ti series were likely generated by low degrees of partial melting (e.g., < 10%) of an OIB-like mantle source within the garnet stability field (Xu et al., 2001; Xiao et al., 2003, 2004; Zhou et al., 2006; Wang et al., 2007; Qi et al., 2008).

On the other hand, some workers have emphasized the compositional continuity between the rocks of the high-Ti and low-Ti series in the Panxi region, and proposed that they were derived from compositionally and isotopically heterogeneous sources and that they reflect mixing of magmas from different sources (e.g. sublithospheric mantle, lithospheric mantle and subducted material), which may have been further modified by assimilation of crustal materials (Shellnutt and Jahn, 2011). A similar model was proposed in a recent study to explain the Pb isotopic composition of the melt inclusions within olivine of the picrites in the Dali region (Ren et al., 2017). However, Ren et al. (2017) argued that the primary melts were generated at different depths from a homogeneous pyroxenite mantle source, which was created by mixing of ancient recycled oceanic crust/sediment and peridotite from the lower mantle. Prior to these two studies, Song et al. (2001) proposed a model that involved interaction of the Emeishan mantle plume with an enriched lithospheric mantle that was modified by subduction of an oceanic slab at shallower depths. Kamenetsky et al. (2012) analyzed the compositions of homogenized melt inclusions hosted by primitive olivine in the Binchuan and Yongsheng picrites, and suggested that the diverse spectrum of more differentiated basaltic magmas within the Emeishan LIP could be attributed to numerous parental magma batches that were produced by mixing of two end-member magmas in different proportions derived from a peridotite and garnet pyroxenite mantle source. The presence of a possible pyroxenite mantle component in the source region of the Emeishan LIP has been suggested in several recent studies, because pyroxenite-derived melts could be more enriched in Ni and possibly Cu than those derived from a peridotite mantle (Sobolev et al, 2009). However, clear evidence of a pyroxenite-derived melt component has not yet been obtained from rocks of the Ni-Cu-(PGE) sulfide-bearing, mafic-ultramafic intrusions in the Emeishan LIP.

Distinct mineralization styles in the Emeishan LIP are attributed to different evolutionary paths that the two magma series may have experienced (e.g., Zhou et al., 2008); Ni-Cu-(PGE) sulfide-bearing, mafic-ultramafic intrusions are believed to have a genetic link to the low-Ti series, whereas Fe-Ti oxide-bearing, layered intrusions are thought to be linked to the high-Ti series. The low-Ti picrites in the Na Muoi River region, northern Vietnam, may resemble the primitive magmas of the low-Ti series, and the εNd(t) and γOs(t) values of the least-evolved, low-Ti picrites may represent the initial Nd-Os isotopic compositions of the primitive magmas from which the Ni-Cu-(PGE) sulfide-bearing, mafic–ultramafic intrusions formed. In this scenario, large variations of εNd (t) and γOs(t) for the rocks from the Limahe, Ban Phuc and Jinbaoshan intrusions are consistent with different degrees of crustal contamination in the formation of these bodies (Fig. 12).

6.2. Controls on sulfide saturation of mantle-derived mafic magmas

A general process leading to the formation of a magmatic Ni-Cu-(PGE) sulfide ore deposit is that mantle-derived mafic magma becomes sulfide-saturated and segregates immiscible sulfide melts, which then are concentrated in a restricted site where their abundance is sufficient to constitute ores. Finally, such sulfide melts react with sufficient amounts of magma to elevate their chalcophile element (Ni, Cu and PGE) composition to an economic level (Naldrett, 2004). Experimental work has shown that S contents at sulfide saturation (SCSS) of mafic magmas increase dramatically with decreasing pressure (Wendlandt, 1982; Lesher and Groves, 1986; Mavrogenes and O'Neill, 1999). In such a situation, sulfide saturation could occur either after substantial crystallization in a closed system, or after significant modification via assimilation of S-rich sediments, felsic rocks, carbonates or graphite (Irvine, 1975; Holwell et al., 2007; Lehmann et al., 2007; Seat et al., 2009).

In theory, sulfide saturation in mantle-derived, mafic magmas can be attained during fractionation of magmas because S is incompatible to silicate and oxide minerals during crystallization (Duke and Naldrett, 1978; Naldrett et al., 1984). For example, in order to attain sulfide saturation of a mafic magma with 1000 ppm S, approximately 43% of fractional crystallization is required (Donoghue et al., 2014). However, fractionation of large amounts of olivine from S-undersaturated mafic magma would deplete the magma in Mg and Ni to a low level. Therefore, some external factors are required for the segregation of considerable amounts of sulfides in magmas before significant crystallization of silicate minerals occur (Naldrett, 2004).

Most Ni-Cu-(PGE) sulfide deposits require the addition of sulfur from an external source close to the final emplacement point. Addition of external crustal sulfur to mantle-derived mafic magmas may cause a remarkable increase in S concentration and trigger sulfide super-

saturation, which is especially important to world-class deposits such as Noril'sk, Duluth and Voisey's Bay (Ripley, 1981; Ripley et al., 1999, 2002; Ripley and Li, 2013). Direct evidence for the addition of external crustal sulfur comes from non-mantle S isotopic compositions in sulfide ores (Ripley, 1981; Li et al., 2003). As shown in Fig. 13, sulfides in the sulfide ores from the Baimazhai No.3, Ban Phuc and Jinbaoshan intrusions have $\delta^{34}S$ values distinctly different from the mantle value, indicating the addition of external crustal sulfur in these intrusions. In contrast, sulfides from the rocks of the Fe-Ti oxide-bearing Panzhihua, Taihe and Baima layered intrusions overall have mantle-like $\delta^{34}S$, likely indicating insignificant addition of external crustal sulfur. This is also consistent with insignificant crustal contamination revealed by the Sr-Nd isotopic compositions of the rocks from these intrusions (Zhong et al., 2004, 2011; Zhou et al., 2008; Song et al., 2013).

Sulfides from ores of Ni-Cu-(PGE) sulfide deposits in the Emeishan LIP have highly variable $\delta^{34}S$, indicating that external sulfur may have been sourced from different country rocks. For example, the Baimazhai No.3 intrusion is hosted in the Ordovician meta-sandstones and slates (Fig. 6), whereas the immediate country rocks of the Ban Phuc intrusion are the Devonian schist, quartzite, gneiss, marble, siliceous limestone and amphibolite of the Ta Khoa Formation (Fig. 7). The Jinbaoshan intrusion is hosted in the Devonian interlayered limestone, sandstone and slate (Fig. 9). It is, however, difficult to determine whether crustal sulfur is from the immediate country rocks or from underlying strata through which magmas passed during ascent. One possibility is that the country rocks are pyrite-rich, because pyrite breaks down in the upper crust at ~800 °C, releasing S and giving rise to pyrrhotite. The Devonian strata in the Danba region consist of graphite-bearing marble with abundant pyrite (up to 5%) (Song et al., 2003) (Fig. 3), which may have been incorporated into the upwelling magmas that were emplaced in the Yangliuping magma chamber. However, it is difficult to envisage how large amounts of country rocks can be assimilated by magmas with sufficient superheat to give rise to the amounts of sulfides present in these intrusions.

Not far from the Baimazhai No.3 intrusion, the Yingpanjie intrusion in the Baimazhai-Santaipo area is weakly mineralized, and the sulfides from the disseminated ores of the intrusion have mantle-like $\delta^{34}S$ values (Fig. 13a). This could indicate that the S was mantle-derived, or that the country rocks have average mantle-like $\delta^{34}S$ values (Ripley et al., 2002). A third possibility is that pre-existing crustal S isotopic signatures were erased by mantle-crust S isotope exchange (Ripley and Li, 2003). Given that the Yingpanjie and Baimazhai No. 3 intrusions were emplaced into the same Ordovician strata, it is likely that the mantle-like $\delta^{34}S$ for the sulfides from the Yingpanjie intrusion is original, and that the signature of external crustal sulfur may have been erased by mantle-crust S isotopic exchange process. This interpretation is consistent with the low degrees of crustal contamination in the Yingpanjie intrusion.

S isotopic compositions of sulfides from the Nantianwan intrusion provide a good example of mantle-crust S isotopic exchange. The intrusion is hosted in the Sinian clastic sedimentary rocks and dolomite (Fig. 8). Sulfides from the olivine gabbro in the intrusion have variable $\delta^{34}S$ ranging from +4.8 to +21.4‰, much higher than the mantle value, whereas sulfides from the gabbronorite have relatively restricted $\delta^{34}S$ of +0.8 to +3.4‰, close to the mantle value (Fig. 13b). The olivine gabbro is thought to have formed from olivine- and sulfide-laden crystal mush in a deep-seated magma chamber that were later incorporated into new and primitive magmas and then intruded the gabbronorite in a shallow magma chamber. In contrast, the gabbronorite likely formed from PGE-depleted, evolved magma in the upper part of the deep-seated magma chamber (Wang et al., 2012a,b). Using the new S isotopic dataset presented in this study, we suggest that sulfide saturation induced by the addition of external sulfur probably occurred only locally in the deep-seated magma chamber, and that the crustal S signature may only be recorded in early-formed sulfide droplets that were preserved in the olivine gabbro. Limited addition of external crustal sulfur would be diluted by replenishment of primitive magmas in the deep-seated chamber. Because S isotopic exchange between large amounts of replenished primitive magmas and limited crustal components, the magmas from which the gabbronorite formed retained their mantle-like S isotopic composition. Therefore, although the parental magmas may have assimilated external crustal sulfur, such assimilation occurred only locally and the amount of crustal sulfur was insufficient to cause significant sulfide saturation, resulting in an economically unimportant intrusion.

In summary, S isotopic compositions of sulfides from the rocks and ores of Ni-Cu-(PGE) sulfide-bearing intrusions in the Emeishan LIP indicate that addition of external crustal sulfur played an important role in the sulfide saturation of mantle-derived mafic magmas. On the other hand, sulfides from weakly mineralized or barren intrusions typically show mantle-like S isotopic compositions. Although some crustal sulfur may have been introduced into these intrusions, the limited crustal S signature was likely overprinted by mantle-crustal S isotopic exchange. Therefore, it appears that extensive addition of external crustal sulfur into the magma chamber was needed to form economically important Ni-Cu-(PGE) sulfide-bearing, mafic-ultramafic intrusions in the Emeishan LIP.

6.3. Structural control on the magma plumbing system

The Emeishan LIP has a paucity of large, mafic-ultramafic intrusions with giant Ni-Cu-(PGE) sulfide mineralization. Most of the Ni-Cu-(PGE) sulfide deposits are hosted in small intrusions with surface outcrops typically less than 1 km^2 (Table 1). This is probably because thrusting and strike-slip faulting are extensively developed in the southwestern margin of the Yangtze Block (Burchfiel et al., 1995) where the Emeishan LIP is well exposed. On a regional scale, significant displacements are recorded on the Xianshuihe and Red River strike-slip faults and several N-S-trending faults have exposed the dykes and intrusions over a considerable range of emplacement depths (Zhou et al., 2002) (Fig. 1). Little attention has previously been paid to the morphology of these magma chambers and conduits. However, a recent study by Lightfoot and Evans-Lamswood (2015) has provided new insights into the structural features that controlled the primary distribution of the Ni-Cu-(PGE) sulfide-bearing intrusions in the Emeishan LIP.

Ni-Cu-(PGE) sulfide-bearing intrusions in the Emeishan LIP basically show two types of morphology; one is a rhomboid-shaped funnel as seen in cross-sections of the Qingquanshan, Limahe, Baimazhai No.3, Ban Phuc and Zhubu intrusions (Figs. 4–7 and 10), and the other is a dyke-like form as seen in cross-sections of the Yangliuping and Jinbaoshan intrusions (Figs. 3 and 9). The morphology and occurrence of these intrusions were likely controlled by strike-slip transtensional zones and most intrusions are located at jogs or cross-linking structures where the strike-slip displacement is offset (Lightfoot and Evans-Lamswood, 2015). In this fashion, the displacement of strike-slip faults may reactivate pre-existing structures in the crust and create local transtensional spaces that guide magma from the mantle to shallower levels (Lightfoot et al., 2012a; Lightfoot and Evans-Lamswood, 2015). This interpretation is consistent with field observations showing that numerous coeval and co-genetic, mafic-ultramafic intrusions commonly occur in the same region, such as those in the Danba and Jinping regions (Figs. 3 and 6). Each of the intrusions can be interpreted as a part of an open plumbing system characterized by channels or conduits (cf., Lightfoot and Evans-Lamswood, 2015; Tao et al., 2015).

We note that Ni-Cu-(PGE) sulfide-bearing intrusions in the Emeishan LIP have high volume ratios of sulfide to silicate melts and the sulfide ores have relatively high Ni, Cu and PGE tenors (Table 1). For example, at least 70% of the Baimazhai No.3 intrusion is mineralized with an average of 54 wt% sulfide in the net-textured and massive ores (Wang and Zhou, 2006), however, the parental magma of the intrusion is estimated to contain only ~0.39 wt% sulfides, indicating that a large portion of the sulfides cannot have accumulated and

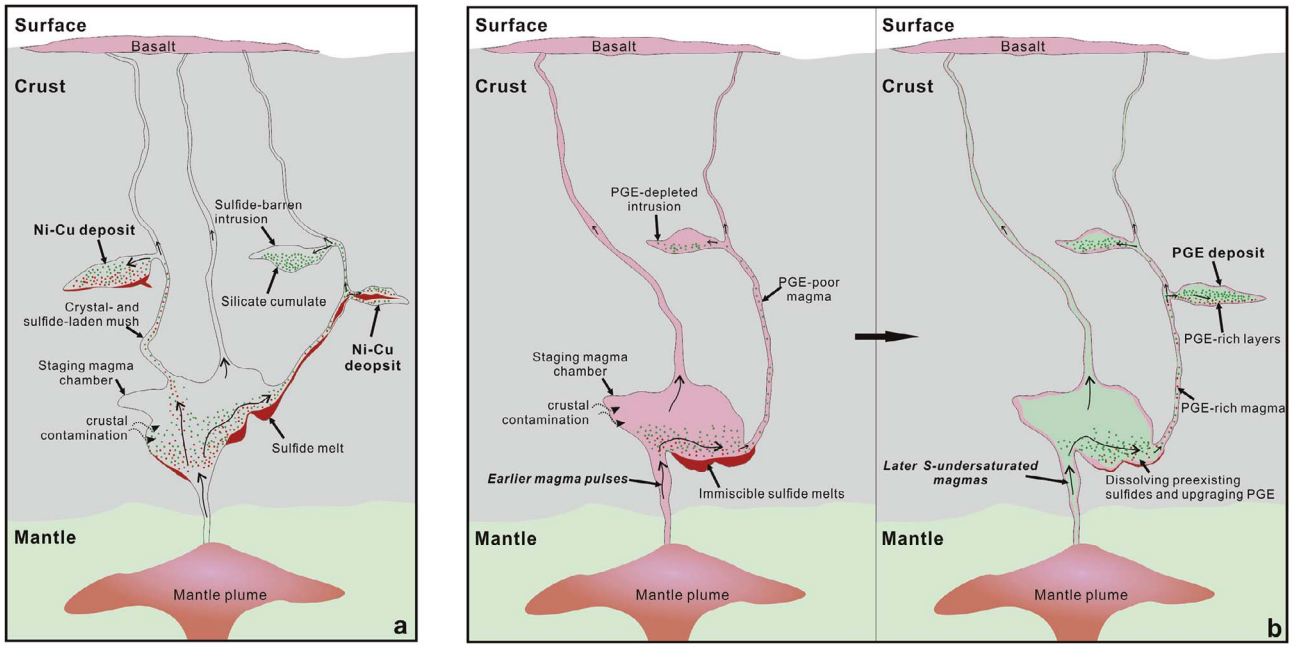

Fig. 15. Schematic models showing the formation of Ni-Cu sulfide-dominated deposits and PGE-dominated deposits in magma conduits, particularly for the formation of economic Ni-Cu-(PGE) sulfide deposits in small, mafic-ultramafic intrusions of the Emeishan LIP (see text for discussion).

segregated *in situ* from the volume of silicate magma present in the current intrusion (cf., Naldrett et al., 1995). In theory, the enrichment of sulfides in PGE, Ni, and Cu requires equilibration of sulfide melt with much larger amounts of silicate melt, which is known as the "R factor", or the ratio of the mass of silicate magma to the mass of sulfide melt (Campbell and Naldrett, 1979), When R is low, the PGE concentration of the ores will be low, and when R is high, PGE concentrations of the ores will be much higher. This is because the partition coefficients of PGE between sulfide and silicate melts vary from 10^4 to 10^6 (Peach et al., 1994; Bezmen et al., 1994; Fleet et al., 1996). The mineralization thus requires an open conduit system where either large amounts of silicate magma can equilibrate with sulfide (Naldrett et al., 1992, 1995) or the sulfide melts can be transported either as sulfide droplets within silicate magmas or moved as dense massive sulfide liquid by tectonic pumping (Naldrett et al., 1992, 1995; Naldrett and Lightfoot, 1999; Bremond d'Ars et al., 2001; Lightfoot et al., 2012a,b). This may explain why one or two economically important intrusions are always associated with a number of barren intrusions in a local region. For example, more than 20 small, mafic-ultramafic intrusions occur in the Jinping region, but only the Baimazhai No.3 intrusion is economically important; other intrusions nearby are mostly weakly mineralized or sulfide-barren (Wang and Zhou, 2006) (Fig. 6a). The same observation applies to the Danba and Huili regions (Figs. 3 and 4). We consider that the barren intrusions are likely the intrusive analogues of Ni-Cu-(PGE)-depleted, residual magma after sulfide segregation in deep-seated magma chambers. When sulfide-saturated magmas are tectonically pumped out of the deep-seated magma chambers and ascend upward to the final magma chamber at shallower level through complex conduits, sulfide- and crystal-laden magma and residual magma may remain in some parts of the conduits. Thus, barren intrusions are unlikely to have any significant potential at depth. On the basis of exploration experience in Sudbury, Lightfoot (2016) concluded that the exploration risks are normally low when exploring near an active part of a mine, but increase significantly even in favorable geological environments outside of the immediate mine environment. The risks are typically very high when exploring a new belt where there is little or no known mineralization. We consider such a principle would also be applicable for exploration in the Emeishan LIP.

Available evidence indicates that magma migration is controlled by a process of tectonic pumping which transfers sulfide-, crystal- and fragment-laden magma and possibly sulfide melts into a final resting place through open system passageways (Lightfoot et al., 2012a,b; Lightfoot and Evans-Lamswood, 2015). Apparently, such pumping cannot be achieved through vertical conduits because of the significant differences in density and viscosity of silicate and sulfide melts (de Bremond d'Ars et al., 2001). However, the presence of gently plunging channels with staging chambers offers an alternative to this problem (Lightfoot and Evans-Lamswood, 2015). In the Emeishan LIP, the principal pathways are commonly associated with sub-vertical, mantle-penetrating structures (cf., Lightfoot and Evans-Lamswood, 2015 and references therein). This may have allowed lateral flow of the sulfide melts so that some sulfide veins may have intruded the host rocks at the base of the intrusion, as observed in the Limahe, Baimazhai No.3 and Ban Phuc intrusions (Figs. 5b and 11b and d). This is similar to the model of a mobilized cumulate slurry in a large, slow-cooling, subsiding magma chamber proposed for the formation of PGE-, Cr- and V-rich layers in the Bushveld Complex (Maier et al., 2013). Therefore, the structural controls may be crucial to the potential target intrusions in the Emeishan LIP. It would be very helpful to map the distribution of strike-slip faults within the Emeishan LIP to decipher the possible conduit systems.

7. An integrated model for Ni-Cu-(PGE) sulfide mineralization in the Emeishan LIP

Ni-Cu-(PGE) sulfide deposits in the Emeishan LIP can be taken as a spectrum of mineralization, the formation of which involved similar magmatic processes in an open system of magma conduits. One end-member in the spectrum is the Baimazhai No.3 intrusion, which is Ni-Cu sulfide-dominated and PGE-depleted; the other is the Jinbaoshan intrusion, which is sulfide-poor and PGE-dominated. Other intrusions in the spectrum have sulfide contents and PGE tenors between these two end-members (Fig. 14b).

An integrated model is shown in Fig. 15 to illustrate the magmatic processes that formed the Ni-Cu-(PGE) sulfide deposits in the Emeishan LIP. The magma conduits were developed along cross-linking structures created by a number of strike-slip faults in the southwestern margin of the Yangtze Block. Each intrusion appears to be part of a connecting

trellis of intrusions and conduits which formed a complex pathway from the mantle to the surface (Lightfoot and Evans-Lamswood, 2015). Early S-undersaturated mafic magma pulses may have reached sulfide saturation due to varying degrees of crustal contamination and fractionation of olivine and chromite, resulting in immiscible sulfide liquid segregated in a deep-seated staging magma chamber (Wang and Zhou, 2006; Tao et al., 2008; Wang et al., 2010). Addition of external crustal sulfur from adjacent or underlying country rocks into magmas is another way to trigger sulfide saturation of the magmas, although this is thought to happen in shallow chambers (e.g., Tao et al., 2008; Wang et al., 2012a,b). The staging chambers subsequently become conduits for later magma incursions. In the Emeishan LIP there likely were gently plunging channels with staging chambers so that massive-sulfide or crystal- and sulfide-laden mush could have been transported from staging chambers to the emplacing chambers at shallower levels (cf., Lightfoot and Evans-Lamswood, 2015). Such a general model can explain the magmatic processes required to form the Ni-Cu-(PGE) sulfide-bearing intrusions in the Emeishan LIP.

A key question in this model is how frequently the multiple magma pulses flow through the staging magma chamber and react with early-segregated, sulfide melts, resulting in different R-factors for each of the intrusions. Similar Pd/Pt and Cu/Pd ratios of the rocks and ores in the Baimazhai No.3 intrusion indicate a single sulfide segregation event in the deep-seated, staging chamber, resulting in the observed depletion of PGE (Wang and Zhou, 2006). It is likely that the immiscible sulfide melts along with residual silicate melts that had volumes much larger than the sulfide melts, were eventually evacuated from the staging magma chamber by compressive forces. Flow differentiation at high velocity is thought to have concentrated the sulfide melts toward the middle of the chamber, and consequently, formed a massive sulfide ore body in the central part of the intrusion. The fractionated carrier magma, i.e., the residual silicate melts, may have been emplaced elsewhere to form the intrusions with distinct signatures of crustal contamination and depletion of Ni, Cu and PGE, i.e., two weakly mineralized intrusions (No.1 and 2) close to the Baimazhai No.3 intrusion (Fig. 6a). The R-factor for the Baimazhai No. 3 intrusion was ~70 (Wang and Zhou, 2006), so the large mass fraction of sulfide melt indicates an absence of multiple magma pulses through the staging chamber and substantial reaction between the sulfide melt and S-undersaturated primary magma. This model can be also used to explain the formation of the Ban Phuc and Limahe intrusions, although a two-stage sulfide segregation model has also been proposed to explain the PGE depletion of the sulfide ores of the Limahe intrusion (Tao et al., 2008). According to our model, the proportion of segregated immiscible sulfide melts in the staging magma chamber of the Limahe intrusion may have been less than that for Baimazhai No.3 intrusion, so it would have been a crystal- and sulfide-laden mush rather than a sulfide melt that was evacuated from the staging chamber. Turbulence and convection in the shallower chamber may have caused settling and sorting of sulfide and crystals in the chamber so that the dense sulfides and olivine crystals eventually settled toward the base of the intrusion, and decreased more or less systematically toward the top of the intrusion (Fig. 15a).

On the other hand, the Jinbaoshan intrusion was formed from PGE-rich magmas that likely resulted from a multistage-dissolution upgrading process in the staging magma chamber (Wang et al., 2010). It is likely that successive pulses of S-undersaturated magma passing through the staging chamber stirred up the sulfide liquids, upgraded them in PGE and incorporated some of them. The remaining PGE-rich sulfide liquids would have been pushed out by later pulses of magma and emplaced in an upper magma chamber to form the Jinbaoshan intrusion (Fig. 15b). In this case, a cumulative R-factor of ~16,000 was obtained in the multistage-dissolution upgrading to produce the high PGE concentrations of the rocks (Wang et al., 2010). This process is analogous to the most intriguing model for the Merensky Reef of the Bushveld Complex, in which a PGE-rich magma is thought to have resulted from multistage dissolution of preexisting sulfides by sulfide-undersaturated magmas (Kerr and Leitch 2005; Naldrett et al., 2009).

The Yangliuping and Qingkuangshan intrusions can be attributed to limited magma pulses passing through the staging magma chambers and limited reaction of early-segregated sulfide melts with S-undersaturated silicate magmas. Song et al. (2003) proposed that fractional crystallization of parental magma accompanied by the introduction of S and CO_2 from the wall rocks caused the magma of the Yangliuping intrusion to become sulfide-saturated, leading to the segregation of sulfides enriched in Ni, Cu and PGE. The sills acted as conduits for the overlying basalts of the Dashibao Formation and sulfide liquids, along with early crystallizing olivine and pyroxene, segregated from the magma as it passed through the conduits prior to eruption. Our model is consistent with the model proposed by Song et al. (2003), and we emphasize the importance of reaction between sulfide melts and limited silicate magma pulses in the staging magma chambers. This is supported by the R values for Ni-Cu-(PGE) sulfide-bearing intrusions in the Emeishan LIP (Song et al., 2008b); the Yangliuping intrusion is calculated to have had a R-factor from 5000 to < 1000, which is between the higher value for Jinbaoshan (1000–100,000) and lower value for Baimazhai (300–2000) (Song et al., 2008b). The Qingkuangshan intrusion has similar features to the Yangliuping intrusion and it may have formed in a similar way.

8. Conclusions

Ni-Cu-(PGE) sulfide deposits in the Emeishan LIP, all of which formed by similar magmatic processes in systems of open magma conduits, can be taken as a spectrum of mineralization associated with mafic-ultramafic intrusions. The magma conduits were developed along cross-linking structures created by a number of strike-slip faults and each intrusion appears to be part of a connecting trellis of intrusions and conduits that formed complex pathways from the mantle to the surface.

The Ni-Cu-(PGE) sulfide-bearing mafic-ultramafic intrusions in the Emeishan LIP may have been derived from similar, low-Ti picritic magma that was generated by relatively high degrees of partial melting of a depleted mantle source around the spinel-garnet transition zone. Assimilation of felsic crustal material and addition of external crustal sulfur were key factors controlling sulfide saturation of mantle-derived mafic magmas in the deep-seated, staging chambers. The staging chambers subsequently became magma conduits for later magma incursions. Gently plunging channels with staging chambers made it possible for massive-sulfide or crystal- and sulfide-laden mush to be transported from the staging to the emplacement chambers at shallower levels. Variations of PGE and sulfide contents of the sulfide ores are attributed to different R-factors of the intrusions, which were related to reaction between early-segregated sulfide melts and progressively replenished S-undersaturated and Ni-Cu-PGE-undepleted mafic magmas that flowed through the staging chambers. The Ni-Cu sulfide-dominated intrusions are attributed to single sulfide segregation events with low R factors in the staging chambers, whereas PGE-dominated intrusions are attributed to multistage-dissolution upgrading events with high R factors.

Acknowledgements

This study was supported by NSFC grants No. 41325006 and 41403037, and the Strategic Priority Research Program (B) of a Chinese Academy of Sciences Grant No. XDB 18000000. Thanks are extended to the reviewer, Paul Robinson and the editor, Jianfeng Gao, for their comments on the manuscript. Paul Robinson also helped to polish the English of the manuscript. Thanks Edward Ripley and Chusi Li for their kind help for S isotope analyses of the Ban Phuc samples.

References

Ali, J.R., Fitton, J.G., Herzberg, C., 2010. Emeishan large igneous province (SW China) and the mantle-plume up-doming hypothesis. J. Geol. Soc. 167, 953–959.

Anh, T.V., Pang, K.N., Chung, S.L., Lin, H.M., Tran, T.H., Tran, T.A., Yang, H.J., 2011. The Song Da magmatic suite revisited: a petrologic, geochemical and Sr–Nd isotopic study on picrites, flood basalts and silicic volcanic rocks. J. Asian Earth Sci. 42, 1341–1355.

Arndt, N.T., Czamanske, G.K., Walker, R.J., Chauvel, C., Fedorenko, V.A., 2003. Geochemistry and origin of the intrusive hosts of the Noril'sk-Talnakh Cu-Ni-PGE sulfide deposits. Econ. Geol. 98, 495–515.

Arne, D., Worley, B., Wilson, C., Fa, C.S., Foster, D., Li, L.Z., Gen, L.S., Dirks, P., 1997. Differential exhumation in response to episodic thrusting along the eastern margin of the Tibetan Plateau. Tectonophysics 280, 239–256.

Barnes, S.-J., Maier, W.D., 1999. The fractionation of Ni, Cu and the noble metals in silicate and sulfide liquids. In: Keays, R.R., Lesher, C.M., Lightfoot, P.C., Farrow, C.E.G. (Eds.), Dynamic Processes in Magmatic Ore Deposits and their Application to Mineral Exploration. Geological Association of Canada, Short Course Notes 13: pp. 69–106.

Bezmen, N.S., Asif, M., Brugmann, G.E., Romanenko, I.M., Naldrett, A.J., 1994. Experimental determinations of sulfide-silicate partitioning of PGE and Au. Geochim. Cosmochim. Acta 58, 1251–1260.

Bremond d'Ars, J., Arndt, N.T., Hallot, E., 2001. Analog experimental insights into the formation of magmatic sulphide deposits. Earth Planet. Sci. Lett. 186, 371–381.

Burchfiel, B.C., Chen, Z., Liu, Y., Royden, L.H., 1995. Tectonics of the Longmen Shan and adjacent regions, central China. Int. Geol. Rev. 37, 661–735.

Campbell, I.H., Naldrett, A.J., 1979. The influence of silicate:sulphide ratios on the geochemistry of magmatic sulfides. Econ. Geol. 74, 1503–1505.

Chung, S.L., Jahn, B.M., 1995. Plume–lithosphere interaction in generation of the Emeishan flood basalts at the Permian-Triassic boundary. Geology 23, 889–892.

Chung, S.L., Jahn, B.M., Wu, G.Y., Lo, C.H., Cong, B.L., 1998. The Emeishan flood basalt in SW China: a mantle plume initiation model and its connection with continental break-up and mass extinction at the Permian–Triassic boundary, In: Flower, M.F.J., Chung, S.L., Lo, C.H., Lee, T.Y. (Eds.), Mantle Dynamics and Plate Interaction in East Asia. American Geophysical Union Geodynamic Series 27, pp. 47–58.

Chung, S.L., Lee, T.L., Lo, C.H., Wang, P.L., Chen, C.Y., Yem, N.T., Hoa, T.T., Wu, G.Y., 1997. Intraplate extension prior to continental extrusion along the Ailao Shan-Red River shear zone. Geology 25, 311–314.

Donoghue, K.A., Ripley, E.M., Li, C.S., 2014. Sulfur isotope and mineralogical studies of Ni-Cu sulfide mineralization in the Bovine Igneous Complex Intrusion, Baraga Basin, Northern Michigan. Econ. Geol. 109, 325–341.

Duke, J.M., Naldrett, A.J., 1978. A numerical model of the fractionation of olivine and molten sulfide from komatiite magma. Earth Planet. Sci. Lett. 39, 255–266.

Ernst, R.E., Jowitt, S.M., 2013. Large igneous provinces (LIPs) and metallogeny, In: Colpron, M., Bissig, T., Rusk, B.G., Thompson, J.F.H. (Eds.), Tectonics, Metallogeny, and Discovery: The North American Cordillera and Similar Accretionary Settings. Society of Economic Geologists Special Publication 17, pp. 17–51.

Fleet, M.E., Crocket, J.H., Stone, W.E., 1996. Partitioning of platinum-group elements (Os, Ir, Ru, Pt, Pd) and gold between sulfide liquid and basalt melt. Geochim. Cosmochim. Acta 60, 2397–2412.

Glotov, A.I., Polyakov, G.V., Hoa, T.T., Balykin, P.A., Akimtsev, V.A., Krivenko, A.P., Tolstykh, N.D., Phuong, N.T., Thanh, H.H., Hung, T.Q., Petrova, T.E., 2001. The Ban Phuc Ni-Cu-PGE deposit related to the Phanerozoic komatiite-basalt association in the Song Da rift, northwestern Vietnam. Can. Mineral. 39, 573–589.

Guan, T., Huang, Z.L., Xie, L.H., Xu, C., Li, W.B., 2003. Geochemistry of lamprophyres in Baimazhai nickel deposit, Yunnan Province: I. major and trace elements. Acta Mineral. Sinica 23, 278–288 (in Chinese with English abstract).

Hanski, E., Walker, R.J., Huhma, H., Polyakov, G.V., Balykin, P.A., Hoa, T.T., Phuong, N.T., 2004. Origin of the Permian-Triassic komatiites, northwestern Vietnam. Contrib. Miner. Petrol. 147, 453–469.

Hanski, E., Kamenetsky, V.S., Luo, Z.Y., Xu, Y.G., Kuzmin, D.V., 2010. Primitive magmas in the Emeishan Large Igneous Province, southwestern China and northern Vietnam. Lithos 119, 75–90.

Hawkesworth, C.J., Lightfoot, P.C., Fedorenko, V.A., Blake, S., Naldrett, A.J., Doherty, W., Gorbachev, N.S., 1995. Magma differentiation and mineralization in the Siberian continental basalts. Lithos 34, 61–88.

He, B., Xu, Y.G., Chung, S.L., Xiao, L., Wang, Y., 2003. Sedimentary evidence for a rapid kilometer-scale crustal doming prior to the eruption of the Emeishan flood basalts. Earth Planet. Sci. Lett. 213, 391–405.

Holwell, D.A., Boyce, A.J., McDonald, I., 2007. Sulfur isotope variations within the Platreef Ni-Cu-PGE deposit: Genetic implications for the origin of sulfide mineralization. Econ. Geol. 102, 1091–1110.

Hou, T., Zhang, Z.C., Encarnacion, J., Santosh, M., Sun, Y.L., 2013. The role recycled oceanic crust in magmatism and metallogenesis: Os-Sr-Nd isotopes, U-Pb geochronology and geochemistry of picritic dykes in the Panzhihua giant Fe-Ti oxide deposit, central Emeishan large igneous province. Contrib. Miner. Petrol. 165, 805–822.

Irvine, T.N., 1975. Crystallization sequences of the Muskox intrusion and other layered intrusions: II. Origin of the chromite layers and similar deposits of other magmatic ores. Geochimicaet Cosmochim. Acta 39, 991–1020.

Kamenetsky, V.S., Chung, S.L., Kamenetsky, M.B., Kuzmin, D.V., 2012. Picrites from the Emeishan Large Igneous Province, SW China: a compositional continuum in primitive magmas and their respective mantle sources. J. Petrol. 53, 2095–2113.

Kerr, A., Leitch, A.M., 2005. Self-destructive sulfide segregation systems and the formation of high-grade magmatic ore deposits. Econ. Geol. 100, 311–332.

Labidi, J., Cartigny, P., Moreira, M., 2013. Non-chondritic sulphur isotope composition of the terrestrial mantle. Nature 501, 208–211.

Le Van De, 1995. Outline of mineral resources and some ideas on mineral development of Vietnam. In: Proceedings of International Symposium: Geology of Southeast Asia and Adjacent Areas. Journal of Geology Special Issue, Series B 5–6, pp. 364–369.

Lehmann, J., Arndt, N.T., Windley, B., Zhou, M.F., Wang, C.Y., Harris, C., 2007. Field relationships and geochemical constraints on the emplacement of the Jinchuan intrusion and its Ni-Cu-PGE sulfide deposit, Gansu, China. Econ. Geol. 102, 75–94.

Lesher, C.M., Groves, D.I., 1986. Controls on the formation of komatiite-associated nickel-copper sulfide deposits: geology and metallogenesis of copper deposits. In: Proceedings of the Twenty-Seventh International Geological Congress. Springer Verlag, Berlin, pp. 43–62.

Li, C., Ripley, E.M., Naldrett, A.J., 2003. Compositional variations of olivine and sulfur isotopes in the Noril'sk and Talnakh intrusions, Siberia: Implications for ore-forming processes in dynamic magma conduits. Econ. Geol. 98, 69–86.

Li, H.B., Zhang, Z.C., Santosh, M., Lü, L.S., Han, L., Liu, W., 2017. Late Permian basalts in the Yanghe area, eastern Sichuan Province, SW China: Implications for the geodynamics of the Emeishan flood basalt province and Permian global mass extinction. J. Asian Earth Sci. 134, 293–308.

Li, J., Xu, J.F., Suzuki, K., He, B., Xu, Y.G., Ren, Z.Y., 2010. Os, Nd and Sr isotope and trace element geochemistry of the Muli picrites: insights into the mantle source of the Emeishan Large Igneous Province. Lithos 119, 108–122.

Lightfoot, P.C., Keays, R.R., 2005. Siderophile and chalcophile metal variations in flood basalts from the Siberian Trap, Noril'sk region: Implications for the origin of the Ni-Cu-PGE sulfide ores. Econ. Geol. 100, 439–462.

Lightfoot, P.C., Keays, R.R., Evans-Lamswood, D., Wheeler, R., 2012a. S saturation history of Nain Plutonic Suite mafic intrusions: origin of the Voisey's Bay Ni–Cu–Co sulfide deposit, Labrador, Canada. Miner. Deposita 47, 23–50.

Lightfoot, P.C., Evans-Lamswood, D., Wheeler, R., 2012b. The Voisey's Bay Ni-Cu-Co sulfide deposit, Labrador, Canada: Emplacement of silicate and sulfide-laden magmas into spaces created within a structural corridor. Northwest Geol. 45, 17–28.

Lightfoot, P.C., Evans-Lamswood, D., 2015. Structural controls on the primary distribution of mafic-ultramafic intrusions containing Ni-Cu-Co-(PGE) sulfide mineralization in the roots of large igneous provinces. Ore Geol. Rev. 64, 354–386.

Lightfoot, P.C., 2016. Nickel Sulfide Ores and Impact Melts: Origin of the Sudbury Igneous Complex. Elsevier, pp. 511–589.

Liu, P.P., Zhou, M.-F., Zhao, G.C., Chung, S.L., Chen, T.W., Wang, F., 2017a. Eocene granulite-facies metamorphism prior to deformation of the Mianhuadi mafic complex in the Ailao Shan-Red River shear zone, Yunnan Province, SW China. J. Asian Earth Sci. 145, 626–640.

Liu, X.J., Liang, Q.D., Li, Z.L., Castillo, P.R., Shi, Y., Xu, J.F., Huang, X.L., Liao, S., Huang, W.L., Wu, W.N., 2017b. Origin of Permian extremely high Ti/Y mafic lavas and dykes from Western Guangxi, SW China: Implications for the Emeishan mantle plume magmatism. J. Asian Earth Sci. 141, 97–111.

Maier, W.D., Barnes, S.J., Groves, D.I., 2013. The Bushveld Complex, South Africa: Formation of platinum–palladium, chrome- and vanadium-rich layers via hydrodynamic sorting of a mobilized cumulate slurry in a large, relatively slowly cooling, subsiding magma chamber. Miner. Deposita 48, 1–56.

Mavrogenes, J.A., O'Neill, H.S.C., 1999. The relative effects of pressure, temperature and oxygen fugacity on the solubility of sulfide in mafic magmas. Geochimicaet Cosmochim. Acta 63 (7), 1173–1180.

Mei, H.J., Xu, Y.G., Xu, J.F., Huang, X.L., He, D.C., 2003. Late Permian basalt–phonolite suite from Longzhoushan in the Panxi rift zone. Acta Geol. Sin. 77, 341–358 (in Chinese with English abstract).

Miller Jr., J.D., Ripley, E.M., 1996. Layered intrusions of the Duluth Complex, Minnesota, USA. In: Cawthorn, R.G. (Ed.), Layered Intrusions. Elsevier, Amsterdam, pp. 257–301.

Mudd, G.M., 2012. Key trends in the resource sustainability of platinum group elements. Ore Geol. Rev. 46, 106–117.

Naldrett, A.J., Duke, J.M., Lightfoot, P.C., Thompson, J.F.H., 1984. Quantitative modeling of the segregation of magmatic sulfides-an exploration guide. Can. Instit. Minerol. Meteorite Bullet. 77, 46–57.

Naldrett, A.J., 1992. A model for the Ni-Cu-PGE ores of the Noril'sk region and its application to other areas of flood basalt. Econ. Geol. 87 (8), 1945–1962.

Naldrett, A.J., Fedorenko, V.A., Lightfoot, P.C., Kunilov, V.E., Gorbachev, N.S., Doherty, W., Johan, Z., 1995. Ni–Cu–PGE deposits of the Noril'sk region Siberia: their formation in conduits for flood basalt volcanism. Trans. Instit. Min. Metall. 104, B18–B36.

Naldrett, A.J., 1997. Key factors in the genesis of Noril'sk, Sudbury, Jinchuan, Voisey's Bay and other world class Ni–Cu–PGE deposits: implications for exploration. Aust. J. Earth Sci. 44, 283–316.

Naldrett, A.J., Lightfoot, P.C., 1999. Ni-Cu-PGE deposits of the Noril'sk region, Siberia; their formation in conduits for flood basalt volcanism. In: Keays, R.R., Lesher, C.M., Lightfoot, P.C., Farrow, C.E.G. (Eds.), Dynamic Processes in Magmatic Ore Deposits and their Application in Mineral Exploration. Geological Association of Canada, Short Course, 13: pp. 195–249.

Naldrett, A.J., 2004. Magmatic sulfide deposits: Geology, geochemistry and exploration. Germany, Springer Verlag, Berlin, pp. 1–727.

Naldrett, A.J., Wilson, A., Kinnaird, J., Chunnett, G., 2009. PGE tenor and metal ratios within and below the Merensky Reef, Bushveld Complex: implications for its genesis. J. Petrol. 50 (4), 625–659.

Naldrett, A.J., 2010a. Secular variation of magmatic sulfide deposits and their source magmas. Econ. Geol. 105 (3), 669–688.

Naldrett, A.J., 2010b. From the mantle to the bank: the life of a Ni–Cu–(PGE) sulfide deposit. S. Afr. J. Geol. 113 (1), 1–32.

Naldrett, A.J., 2011. Fundamentals of magmatic sulfide deposits, In: Li, C., Repley, E.M. (Eds.), Magmatic Ni-Cu and PGE Deposits: Geology, Geochemistry, and Genesis. Society of Economic Geology Special Publication 17, pp. 1–26.

Peach, C.L., Mathez, E.A., Keays, R.R., Reeves, S.J., 1994. Experimentally determined sulfide melt-silicate melt partition coefficients for Ir and Pd. Chem. Geol. 117, 361–377.
Pirajno, F., 2000. Ore Deposits and Mantle Plumes. Kluwer Academic Publication, pp. 1–556.
Qi, L., Wang, C.Y., Zhou, M.-F., 2008. Controls on the PGE distribution of Permian Emeishan alkaline and peralkaline volcanic rocks in Longzhoushan, Sichuan Province, SW China. Lithos 106 (3), 222–236.
Qi, L., Zhou, M.-F., 2008. Platinum-group elemental and Sr–Nd–Os isotopic geochemistry of Permian Emeishan flood basalts in Guizhou Province, SW China. Chem. Geol. 248, 83–103.
Ren, Z.Y., Wu, Y.D., Zhang, L., Nichols, A.R.L., Hong, L.B., Zhang, Y.H., Zhang, Y., Liu, J.Q., Xu, Y.G., 2017. Primary magmas and mantle sources of Emeishan basalts constrained from major element, trace element and Pb isotope compositions of olivine-hosted melt inclusions. Geochim. Cosmochim. Acta 208, 63–85.
Ripley, E.M., 1981. Sulfur isotopic studies of the Dunka Road Cu-Ni deposit, Duluth Complex, Minnesota. Econ. Geol. 76, 610–620.
Ripley, E.M., Park, Y.R., Li, C.S., Naldrett, A.J., 1999. Sulfur and oxygen isotopic vidence of country rock contamination in the Voisey's Bay Ni-Cu-Co deposit, Labrador, Canada. Lithos 47, 53–68.
Ripley, E.M., Li, C., Shin, D., 2002. Paragneiss Assimilation in the Genesis of Magmatic Ni-Cu-Co Sulfide Mineralization at Voisey's Bay, Labrador: $\delta^{34}S$, $\delta^{13}C$, and Se/S Evidence. Econ. Geol. 97, 1307–1318.
Ripley, E.M., Li, C., 2003. Sulfur isotope exchange and metal enrichment in the formation of magmatic Cu-Ni-(PGE) deposits. Econ. Geol. 98, 635–641.
Ripley, E.M., Li, C., 2013. Sulfide saturation in mafic magmas: Is external sulfur required for magmatic Ni-Cu-(PGE) ore genesis? Econ. Geol. 108, 45–58.
Schissel, D., Smail, R., 2001. Deep-mantle plumes and ore deposits. Geol. Soc. Am. Special Papers 352, 291–322.
Seat, Z., Beresford, S.W., Grguric, B.A., Mary Gee, M.A., Grassineau, N.V., 2009. Reevaluation of the Role of External Sulfur Addition in the Genesis of Ni-Cu-PGE Deposits: Evidence from the Nebo-Babel Ni-Cu-PGE Deposit, West Musgrave, Western Australia. Econ. Geol. 104, 521–538.
Shellnutt, J.G., Jahn, B.M., 2011. Origin of Late Permian Emeishan basaltic rocks from the Panxi region (SW China): Implications for the Ti-classification and spatial-compositional distribution of the Emeishan flood basalts. J. Volcanol. Geoth. Res. 199 (1), 85–95.
Shirey, S.B., Walker, R.J., 1998. The Re-Os isotope system in cosmochemistry and high-temperature geochemistry. Annu. Rev. Earth Planet. Sci. 26, 423–500.
Sobolev, A.V., Krivolutskaya, N.A., Kuzmin, D.V., 2009. Petrology of the parental melts and mantle sources of Siberian trap magmatism. Petrology 17 (3), 253–286.
Song, X.Y., Zhou, M.-F., Wang, Y.L., Zhang, C.J., Cao, Z.M., Li, Y., 2001. Geochemical constrains on the mantle source of the Upper Permian Emeishan continental flood basalts, SW China. Int. Geol. Rev. 43 (3), 213–225.
Song, X.Y., Zhou, M.-F., Cao, Z.M., Sun, M., Wang, Y.L., 2003. Ni-Cu-(PGE) magmatic sulfide deposits in the Yangliuping area, Permian Emeishan igneous province, SW China. Mineralium Deposita 38 (7), 831–843.
Song, X.Y., Zhou, M.-F., Cao, Z.M., Robinson, P.T., 2004a. Late Permian rifting of the South China Craton Caused by the Emeishan Mantle Plume. J. Geol. Soc. 161, 773–781.
Song, X.Y., Zhou, M.-F., Cao, Z.M., 2004b. Genetic relationships between base-metal sulfides and platinum-group minerals in the Yangliuping Ni-Cu-(PGE) sulfide deposit, SW China. Can. Mineral. 42, 469–484.
Song, X.Y., Zhou, M.-F., Keays, R.R., Cao, Z.M., Sun, M., Qi, L., 2006. Geochemistry of the Emeishan flood basalts at Yangliuping, Sichuan, SW China: implications for sulfide segregation. Contrib. Miner. Petrol. 152, 53–74.
Song, X.Y., Qi, H.W., Robinson, P.T., Zhou, M.-F., Cao, Z.M., Chen, L.M., 2008a. Melting of the subcontinental lithospheric mantle by the Emeishan mantle plume; evidence from the basal alkaline basalts in Dongchuan, Yunnan, Southwestern China. Lithos 100, 93–111.
Song, X.Y., Zhou, M.-F., Tao, Y., Xiao, J.F., 2008b. Controls on the metal compositions of magmatic sulfide deposits in the Emeishan large igneous province, SW China. Chem. Geol. 253 (1), 38–49.
Song, X.Y., Qi, H.W., Hu, R.Z., Chen, L.M., Yu, S.Y., Zhang, J.F., 2013. Formation of thick stratiform Fe-Ti oxide layers in layered intrusion and frequent replenishment of fractionated mafic magma: Evidence from the Panzhihua intrusion, SW China. Geochem. Geophys. Geosyst. 14 (3), 712–732.
Studley, S.A., Ripley, E.M., Elswick, E.R., Dorais, M.J., Fong, J., Finkelstein, D., Pratt, L.M., 2002. Analysis of sulfides in whole rock matrices by elemental analyzer–continuous flow isotope ratio mass spectrometry. Chem. Geol. 192 (1–2), 141–148.
Sun, X.M., Wang, S.W., Sun, W.D., Shi, G.Y., Sun, Y.L., Xiong, D.X., Qu, W.J., Du, A.D., 2008. PGE geochemistry and Re–Os dating of massive sulfide ores from the Baimazhai Cu–Ni deposit, Yunnan province, China. Lithos 105 (1–2), 12–24.
Tang, Q.Y., Ma, Y.S., Zhang, M.J., Li, C., Zhu, D., Tao, Y., 2013. The origin of Ni-Cu-PGE sulfide mineralization in the margin of the Zhubu mafic-ultramafic intrusion in the Emeishan large igneous province, SW China. Econ. Geol. 108 (8), 1889–1901.
Tang, Q.Y., Li, C., Tao, Y., Ripley, E.M., Xiong, F., 2017. Association of Mg-rich Olivine with Magnetite as a Result of Brucite Marble Assimilation by Basaltic Magma in the Emeishan Large Igneous Province, SW China. J. Petrol. 58 (4), 699–714.
Tao, Y., Li, C., Hu, R., Ripley, E.M., Du, A., Zhong, H., 2007. Petrogenesis of the Pt–Pd mineralized Jinbaoshan ultramafic intrusion in the Permian Emeishan large igneous province, SW China. Contrib. Miner. Petrol. 153, 321–337.
Tao, Y., Li, C., Song, X.Y., Ripley, E.M., 2008. Mineralogical, petrological, and geochemical studies of the Limahe mafic-ultramatic intrusion and associated Ni-Cu sulfide ores, SW China. Mineralium Deposita 43 (8), 849–872.
Tao, Y., Ma, Y.S., Miao, L.C., Zhu, F.L., 2009. SHRIMP U-Pb zircon age of the Jinbaoshan ultramafic intrusion, Yunnan Province, SW China. Chin. Sci. Bull. 54, 168–172.
Tao, Y., Li, C., Hu, R., Qi, L., Qu, W., Du, A., 2010. Re–Os isotopic constraints on the genesis of the Limahe Ni–Cu deposit in the Emeishan large igneous province, SW China. Lithos 119, 137–146.
Tao, Y., Putirka, K., Hu, R.Z., Li, C.S., 2015. The magma plumbing system of the Emeishan large igneous province and its role in basaltic magma differentiation in a continental setting. Am. Mineral. 100 (11–12), 2509–2517.
Tran Van Tri, 1995. Vietnam's tectonic framework and mineral potential. In: Proc. Int. Symp. Geology of Southeast Asia and Adjacent Areas. Journal of Geology Specical Issue, Series B 5–6, pp. 275–281.
Wang, C.Y., Zhou, M.-F., Zhao, D.G., 2005. Mineral chemistry of chromite from the Permian Jinbaoshan Pt-Pd-sulphide-bearing ultramafic intrusion in SW China with petrogenetic implications. Lithos 83 (1), 47–66.
Wang, C.Y., Zhou, M.-F., 2006. Genesis of the Permian Baimazhai magmatic Ni-Cu-(PGE) sulfide deposit, Yunnan, SW China. Mineralium Deposita 41 (8), 771–783.
Wang, C.Y., Zhou, M.-F., Keays, R.R., 2006. Geochemical constraints on the origin of the Permian Baimazhai mafic–ultramafic intrusion, SW China. Contrib. Miner. Petrol. 152, 309–321.
Wang, C.Y., Zhou, M.-F., Qi, L., 2007. Permian flood basalts and mafic intrusions in the Jinping (SW China)–Song Da (northern Vietnam) district: Mantle sources, crustal contamination and sulfide segregation. Chem. Geol. 243 (3), 317–343.
Wang, C.Y., Prichard, H.Z., Zhou, M.F., Fisher, P.C., 2008. Platinum-group minerals from the Jinbaoshan Pd–Pt deposit, SW China: evidence for magmatic origin and hydrothermal alteration. Miner. Deposita 43, 791–803.
Wang, C.Y., Zhou, M.-F., Qi, L., 2010. Origin of extremely PGE-rich mafic magma system: An example from the Jinbaoshan ultramafic sill, Emeishan Large Igneous Province, SW China. Lithos 119 (1), 147–161.
Wang, C.Y., Zhou, M.-F., Qi, L., 2011. Chalcophile element geochemistry and petrogenesis of high-Ti and low-Ti magmas in the Permian Emeishan large igneous province, SW China. Contrib. Miner. Petrol. 161 (2), 237–254.
Wang, C.Y., Zhou, M.-F., Sun, Y.L., Arndt, N.T., 2012a. Differentiation, crustal contamination and emplacement of magmas in the formation of the Nantianwan mafic intrusion of the ~260 Ma Emeishan large igneous province, SW China. Contrib. Miner. Petrol. 164 (2), 281–301.
Wang, C.Y., Zhou, M.-F., Yang, S.H., Qi, L., Sun, Y.L., 2014. Geochemistry of the Abulangdang intrusion: Cumulates of high-Ti picritic magmas in the Emeishan large igneous province, SW China. Chem. Geol. 378, 24–39.
Wang, M., Zhang, Z.C., Encarnacion, J., Hou, T., Luo, W.J., 2012b. Geochronology and geochemistry of the Nantianwan mafic–ultramafic complex, Emeishan large igneous province: metallogenesis of magmatic Ni-Cu sulphide deposits and geodynamic setting. Int. Geol. Rev. 54, 1746–1764.
Wendlandt, R.F., 1982. Sulfide saturation of basalt and andesite melts at high pressures and temperatures. Am. Mineral. 67, 877–885.
Xiao, L., Xu, Y.G., Chung, S.L., He, B., Mei, H.J., 2003. Chemostratigraphic correlation of Upper Permian lava succession from Yunnan Province, China: Extent of the Emeishan large igneous province. Int. Geol. Rev. 45, 753–766.
Xiao, L., Xu, Y.G., Mei, H.J., Zheng, Y.F., He, B., Pirajno, F., 2004. Distinct mantle sources of low-Ti and high-Ti basalts from the western Emeishan large igneous province, SW China: implications for plume–lithosphere interaction. Earth Planet. Sci. Lett. 228 (3), 525–546.
Xu, Y.G., Chung, S.L., Jahn, B.M., Wu, G.Y., 2001. Petrologic and geochemical constraints on the petrogenesis of Permian-Triassic Emeishan flood basalts in southwestern China. Lithos 58 (3), 145–168.
Xu, Y.G., He, B., Chung, S.L., Menzies, M.A., Frey, F.A., 2004. Geologic, geochemical, and geophysical consequences of plume involvement in the Emeishan flood-basalt province. Geology 32 (10), 917–920.
Yan, D.P., Zhou, M.F., Song, H.L., Fu, Z.R., 2003. Structural style and tectonic significance of the Jianglang metamorphic core complex, eastern margin of the Tibetan Plateau, China. J. Struct. Geol. 5 (5), 765–779.
Zhang, L., Ren, Z.Y., Wang, C.Y., 2017. Melt inclusions in the olivine from the Nantianwan intrusion: Implications for the parental magma of Ni-Cu-(PGE) sulfide-bearing mafic-ultramafic intrusions of the ~260 Ma Emeishan large igneous province (SW China). J. Asian Earth Sci. 134, 72–85.
Zhang, Y.X., Wang, S., 1996. The History of Discovery of Mineral Deposits in China–the Sichuan Province Volume. Geological Publishing House, Beijing, pp. 108–110 (in Chinese).
Zhang, Z.C., Zhi, X.C., Chen, L., Saunders, A.D., Reichow, M.K., 2008. Re–Os isotopic compositions of picrites from the Emeishan flood basalt province, China. Earth Planet. Sci. Lett. 276 (1–2), 30–39.
Zhong, H., Qi, L., Hu, R.Z., Zhou, M.F., Gou, T.Z., Zhu, W.G., Liu, B.G., Chu, Z.Y., 2011. Rhenium-osmium isotope and platinum-group elements in the Xinjie layered intrusion, SW China: Implications for source mantle composition, mantle evolution, PGE fractionation and mineralization. Geochim. Cosmochim. Acta 75 (6), 1621–1641.
Zhong, H., Yao, Y., Prevec, S.A., Wilson, A.H., Viljoen, M.J., Viljoen, R.P., Liu, B.G., Luo, Y.N., 2004. Trace-element and Sr-Nd isotopic geochemistry of the PGE-bearing Xinjie layered intrusion in SW China. Chem. Geol. 203, 237–252.
Zhong, Y.T., He, B., Mundil, R., Xu, Y.G., 2014. CA-TIMS zircon U-Pb dating of felsic ignimbrite from the Binchuan section: Implications for the termination age of the Emeishan large igneous province. Lithos 204, 14–19.
Zhou, M.-F., Arndt, N.T., Malpas, J., Wang, C.Y., Kennedy, A.K., 2008. Two magma series and associated ore deposit types in the Permian Emeishan large igneous province, SW China. Lithos 103 (3), 352–368.
Zhou, M.-F., Chen, W.T., Wang, C.Y., Prevec, S.A., Liu, P.P., Howarth, G.H., 2013. Two stages of immiscible liquid separation in the formation of Panzhihua-type Fe-Ti-V oxide deposits, SW China. Geosci. Front. 4, 481–502.

Zhou, M.-F., Malpas, J., Song, X.Y., Robinson, P.T., Sun, M., Kennedy, A.K., Lesher, C.M., Keays, R.R., 2002. A temporal link between the Emeishan Large Igneous Province (SW China) and the end-Guadalupian mass extinction. Earth Planet. Sci. Lett. 196, 113–122.

Zhou, M.-F., Robinson, P.T., Lesher, C.M., Keays, R.R., Zhang, C.J., Malpas, J., 2005. Geochemistry, petrogenesis, and metallogenesis of the Panzhihua gabbroic layered intrusion and associated Fe-Ti-V-oxide deposits, Sichuan Province, SW China. J. Petrol. 46 (11), 2253–2280.

Zhou, M.-F., Zhao, J.H., Qi, L., Su, W.C., Hu, R.Z., 2006. Zircon U-Pb geochronology and elemental and Sr-Nd isotope geochemistry of Permian mafic rocks in the Funing area, SW China. Contrib. Miner. Petrol. 151, 1–19.

Zhu, D., Xu, Y.G., Luo, T.Y., Song, X.Y., Tao, Y., Huang, Z.L., Zhu, C.M., Cai, E.Z., 2007. Conduit of the Emeishan basalts: the Zhubu mafic-ultramafic intrusion in the Yuanmou area of Yunnan Province, China. Acta Mineral. Sinica 27, 273–280 (in Chinese with English abstract).

Zhu, F.L., Tao, Y., Hu, R.Z., Ma, Y.S., 2012. Geochemical characteristics and metallogenesis of the Qingkuangshan Ni-Cu-PGE mineralized mafic-ultramafic intrusion in Huili County, Sichuan Province, SW China. Acta Geol. Sinica (English edition) 86 (3), 590–607.

Zhu, F.L., Tao, Y., Hu, R.Z., Yu, S.Y., Qu, W.J., Du, A.D., 2011. Re-Os isotopic constraints on the ore-forming mechanism for the Qingkuangshan Ni-Cu-PGE deposit in the Huili County, Sichuan Province. Acta Petrol. Sinica 27 (9), 2655–2664 (in Chinese with English abstract).

Zindler, A., Hart, S., 1986. Chemical geodynamics. Ann. Rev. Earth Planet. Sci. 14, 493–571.